Baryon spectroscopy and new resonances in meson photoproduction experiments

A.V. Anisovich, A.V. Sarantsev

Petersburg Nuclear Physics Institute

N^*- resonances in the quark model

Nukleon

10^{-15} m

U. Loering, B. Metsch, H. Petry et al. (Bonn)

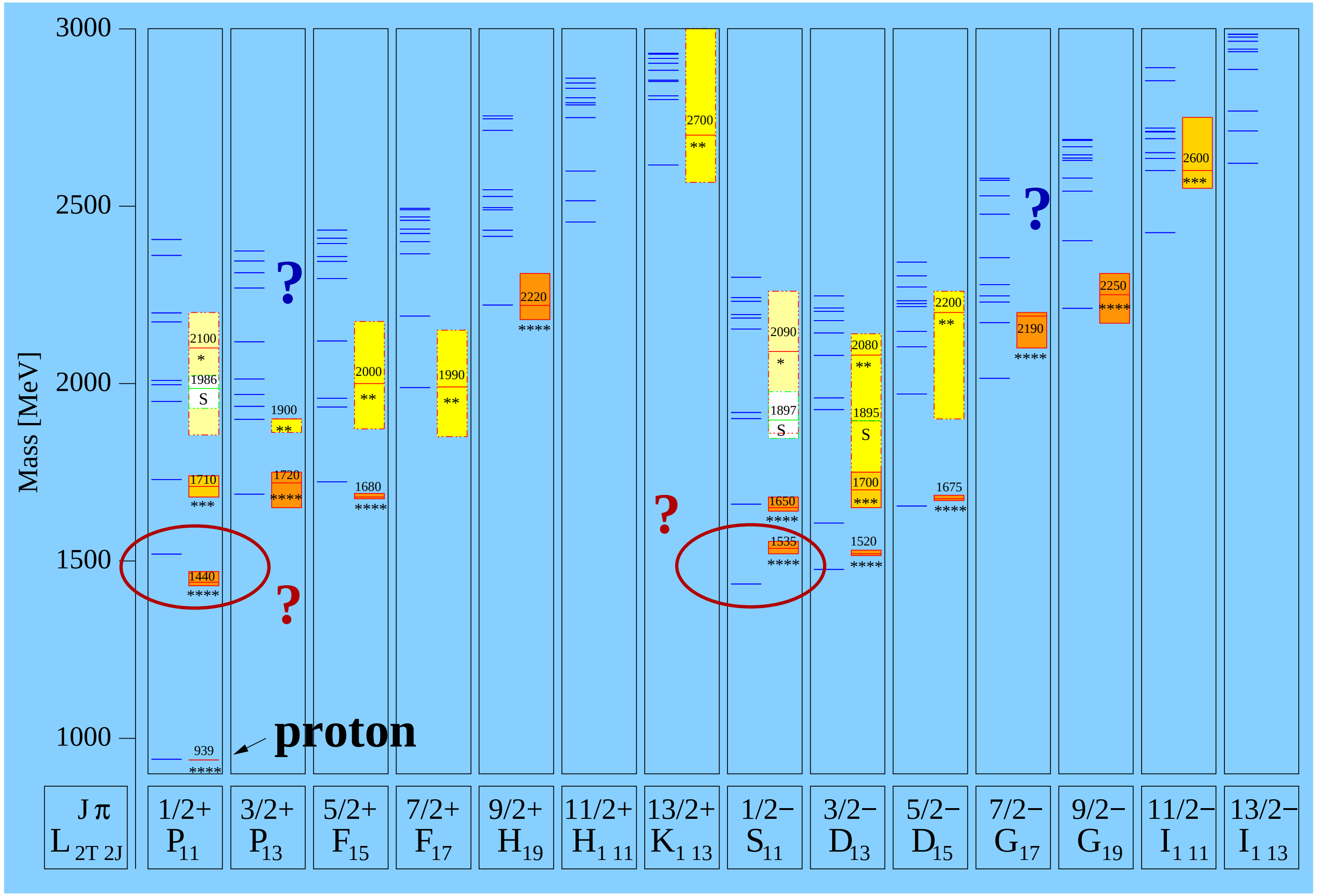

↔

Constituent quarks

Confinement-potential

Residual interaction

The Δ^*- states

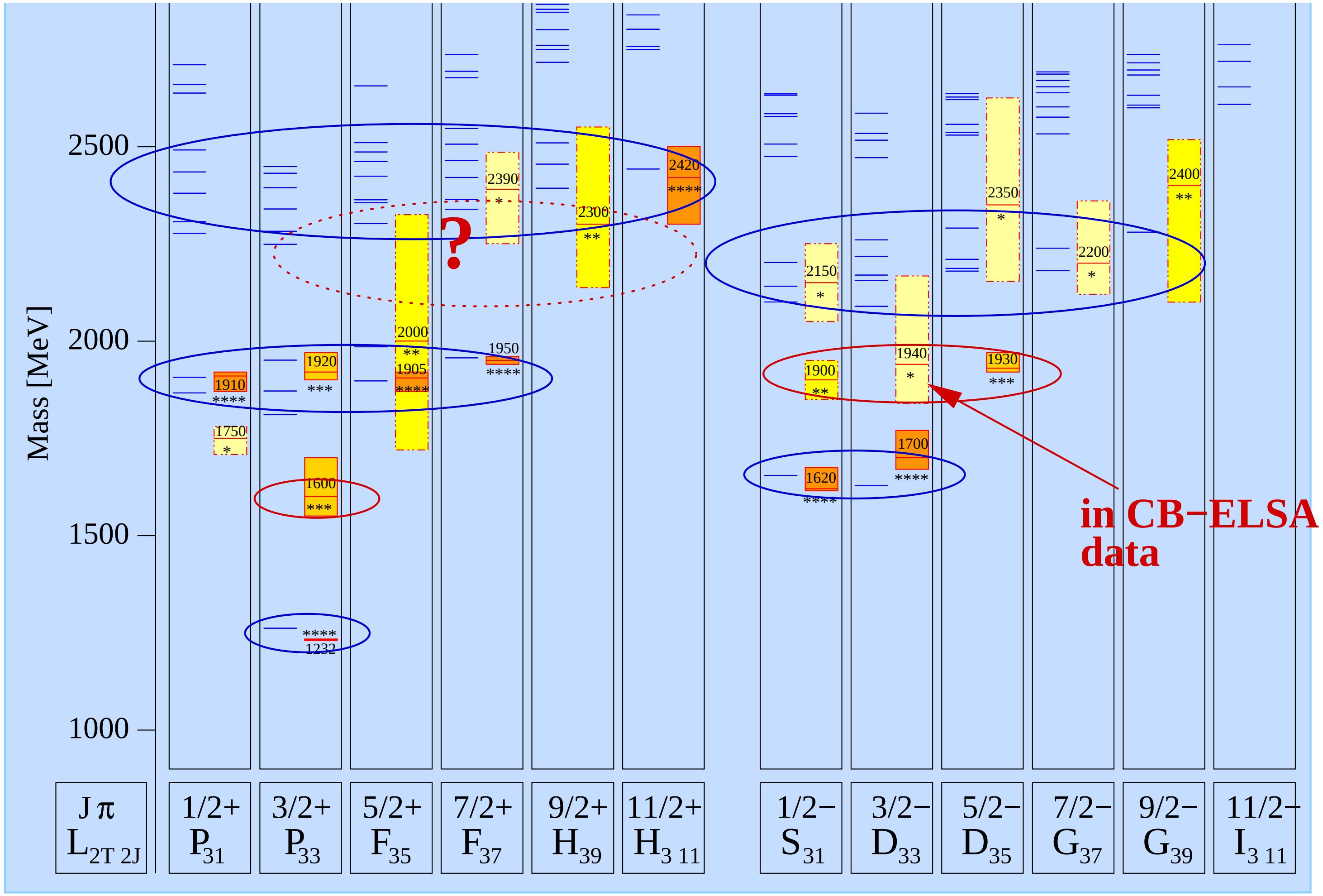

Quark model
U. Löring, B. Metsch,
H. Petry et al.

model
$\sim 2n + \ell$

data
$\sim n + \ell$?

$\leftrightarrow$ **Parity doublets ?**

$\Leftrightarrow$ Additional experimental information needed !!

Problems in the baryon spectroscopy and/or quark model:

1. **Problem: The number of predicted three quark states exceeds dramatically the number of discovered baryons.**

2. **Possible solution: Most of the information comes from the analysis of meson induced reactions and meson-baryon final states. Photoproduction data taken by CLAS, GRAAL, LEPS and CB-ELSA can provide an important information about missing states.**

   (a) **problem: The unambiguous analysis of photoproduction reactions can not be done without polarization information available.**

   (b) **problem: Signals in simple reactions are expected to be mostly weak. Strong signals from new resonances can be found in multi-meson final states.**

   (c) **Possible solution 1: The single polarization observables are measured now by almost all collaborations. In the nearest future single and double polarization data will be available from CLAS and CB-ELSA.**

   (d) **Possible solution 2: A combined analysis of the large data sets.**

For combined analysis of all available data a new approach is needed:

1. **Fully relativistically invariant.**
2. **Convenient for combined analysis of single and multi-meson photoproduction.**
3. **Energy dependent, which allow us to apply directly the unitarity and analyticity conditions.**
4. **Convenient for calculation of the triangle and box diagrams or projection of the t and u-channel exchange amplitudes to the partial waves in s-channel.**

A. Anisovich, E. Klempt, A. Sarantsev and U. Thoma, Eur. Phys. J. A 24, 111 (2005)

A. V. Anisovich and A. V. Sarantsev, Eur. Phys. J. A 30 (2006) 427

A. V. Anisovich, V. V. Anisovich, E. Klempt, V. A. Nikonov and A. V. Sarantsev,

Eur. Phys. J. A 34 (2007) 129.

The fitted reactions with two particle final states.

Observable	$N_{\rm data}$	w_i	$\frac{\chi^2}{N_{\rm data}}$		Observable	$N_{\rm data}$	w_i	$\frac{\chi^2}{N_{\rm data}}$	
$\sigma(\gamma p \to p\pi^0)$	1106	7	0.99	CB-ELSA	$\sigma(\gamma p \to p\pi^0)$	861	3	3.22	GRAAL
$\Sigma(\gamma p \to p\pi^0)$	469	2.3	3.75	GRAAL	$\Sigma(\gamma p \to p\pi^0)$	593	2.3	2.13	SAID
$P(\gamma p \to p\pi^0)$	594	3	2.58	SAID	$T(\gamma p \to p\pi^0)$	380	3	3.85	SAID
$\sigma(\gamma p \to n\pi^+)$	1583	2.8	1.07	SAID					
$\sigma(\gamma p \to p\eta)$	667	30	0.84	CB-ELSA	$\sigma(\gamma p \to p\eta)$	100	7	1.69	TAPS
$\Sigma(\gamma p \to p\eta)$	51	10	1.82	GRAAL 98	$\Sigma(\gamma p \to p\eta)$	100	10	2.11	GRAAL 04
$C_x(\gamma p \to \Lambda K^+)$	160	5	1.71	CLAS	$C_z(\gamma p \to \Lambda K^+)$	160	7	1.95	CLAS
$\sigma(\gamma p \to \Lambda K^+)$	1377	5	2.02	CLAS	$\sigma(\gamma p \to \Lambda K^+)$	720	1	1.53	SAPHIR
$P(\gamma p \to \Lambda K^+)$	202	6.5	1.65	CLAS	$P(\gamma p \to \Lambda K^+)$	66	3	2.89	GRAAL
$\Sigma(\gamma p \to \Lambda K^+)$	66	5	2.19	GRAAL	$\Sigma(\gamma p \to \Lambda K^+)$	45	10	1.98	LEP
$C_x(\gamma p \to \Sigma^0 K^+)$	94	5	2.70	CLAS	$C_z(\gamma p \to \Sigma^0 K^+)$	94	5	2.77	CLAS
$\sigma(\gamma p \to \Sigma^0 K^+)$	1280	3	2.10	CLAS	$\sigma(\gamma p \to \Sigma^0 K^+)$	660	1	1.33	SAPHIR
$P(\gamma p \to \Sigma^0 K^+)$	95	6	1.58	CLAS	$\Sigma(\gamma p \to \Sigma^0 K^+)$	42	5	1.04	GRAAL
$\Sigma(\gamma p \to \Sigma^0 K^+)$	45	10	0.62	LEP	$\sigma(\gamma p \to \Sigma^+ K^0)$	48	2.3	3.51	CLAS
$\sigma(\gamma p \to \Sigma^+ K^0)$	120	5	0.98	SAPHIR	$\sigma(\gamma p \to \Sigma^+ K^0)$	72	5	1.17	CB-ELSA

Three particle final states reactions fitted with maximum likelihood method.

Observable	
$\sigma(\gamma p \to p\pi^0\pi^0)$	**CB-ELSA (1.4 GeV)**
$\sigma(\gamma p \to p\pi^0\pi^0)$	**TAPS**
$\sigma(\gamma p \to p\pi^0\eta)$	**CB-ELSA (3.2 GeV)**
$E(\gamma p \to p\pi^0\pi^0)$	**MAMI**
$\Sigma(\gamma p \to p\pi^0\pi^0)$	**GRAAL**
$\sigma(\pi^- p \to n\pi^0\pi^0)$	**CRYSTAL BALL**

$\gamma p \to \pi^0 p$ from Crystal Barrel at ELSA ($E_\gamma \leq 3.2$ GeV)

$\Delta(1232)P_{33}$
$N(1520)D_{13}\ S_{11}$
$N(1680)F_{15}$
$\Delta(1700)D_{33}$
$\Delta(1920)P_{33}$

Non-resonance contribution:

t-channel $\rho - \omega$ exchange, u-exchange and non-resonance production in $J^P = 3/2^+$ wave

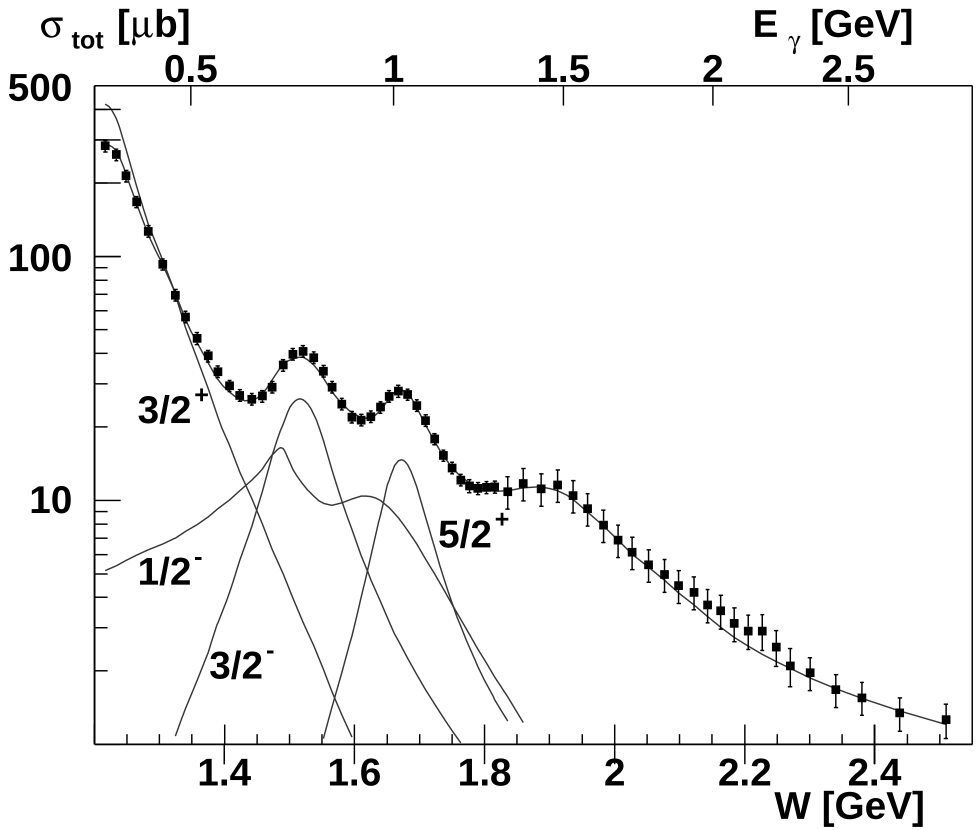

$\gamma p \to \pi^0 p$ from Crystal Barrel at ELSA ($E_\gamma \leq 3.2$ GeV)

$\Delta(1232)P_{33}$, S_{11}, $N(1520)D_{13}$, $N(1680)F_{15}$

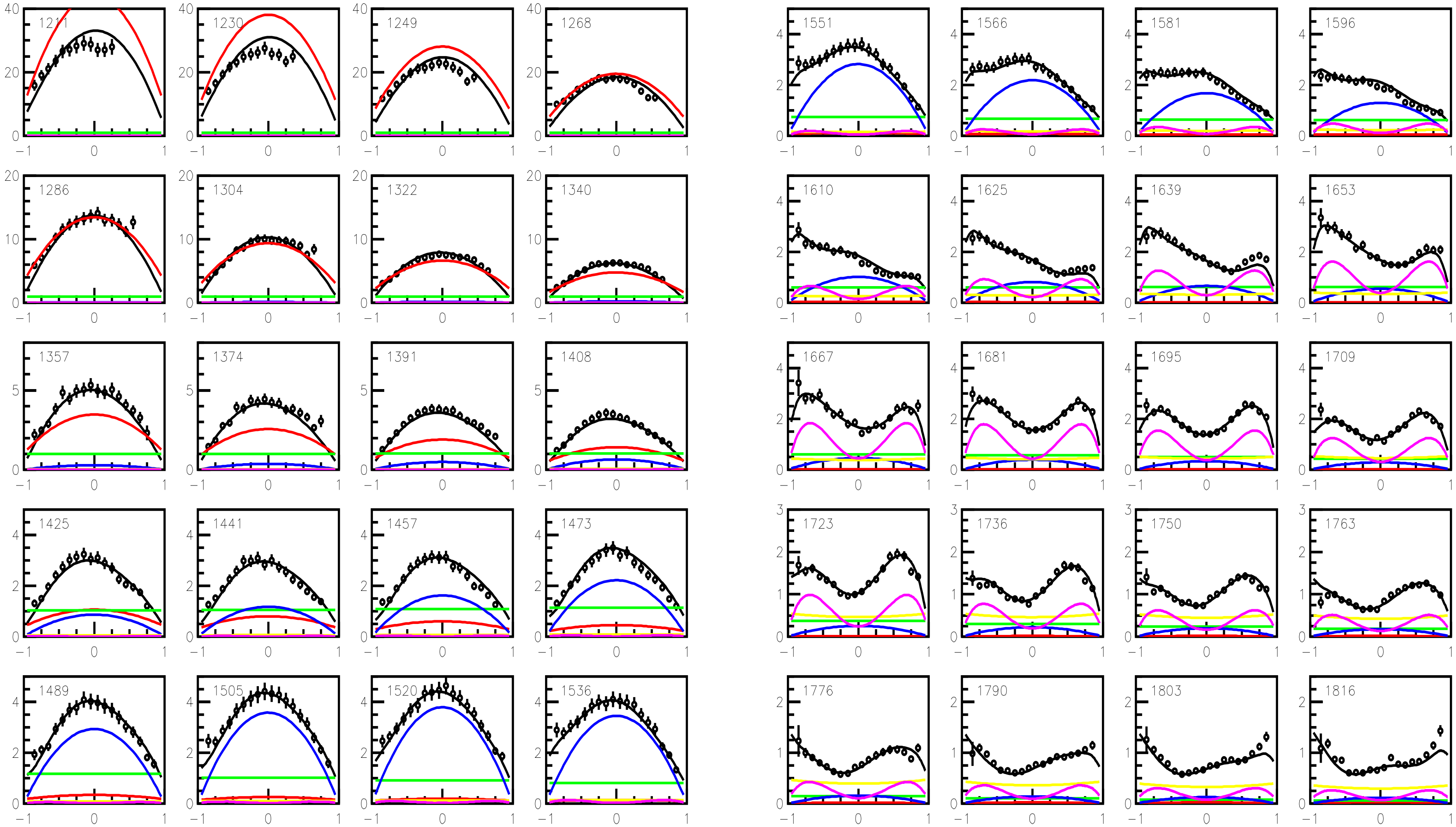

$\gamma p \to \pi^0 p$ from Crystal Barrel at ELSA ($E_\gamma \leq 3.2$ GeV)

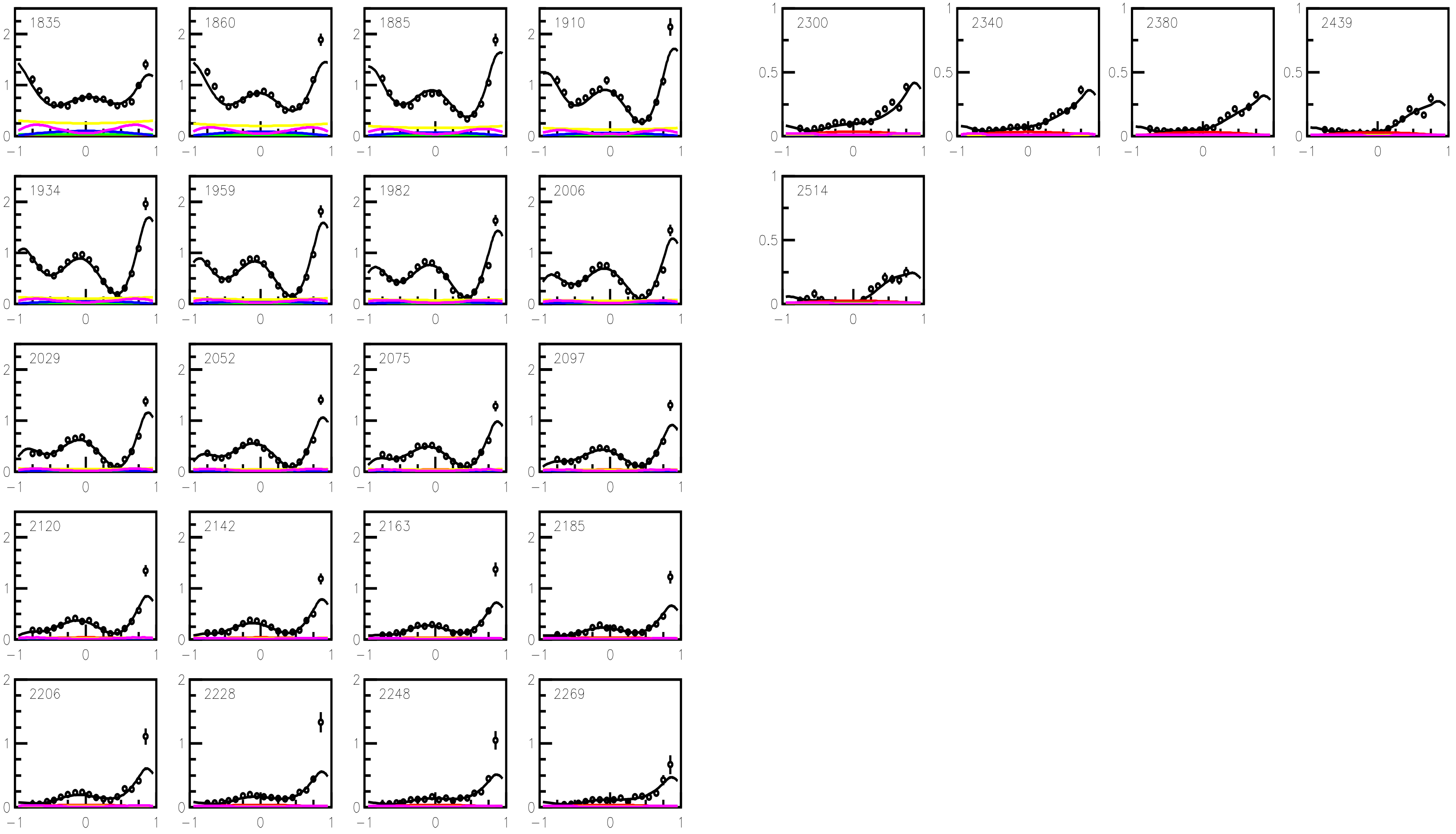

Beam asymmetry $\Sigma(\gamma p \to \pi^0 p)$ from GRAAL 04

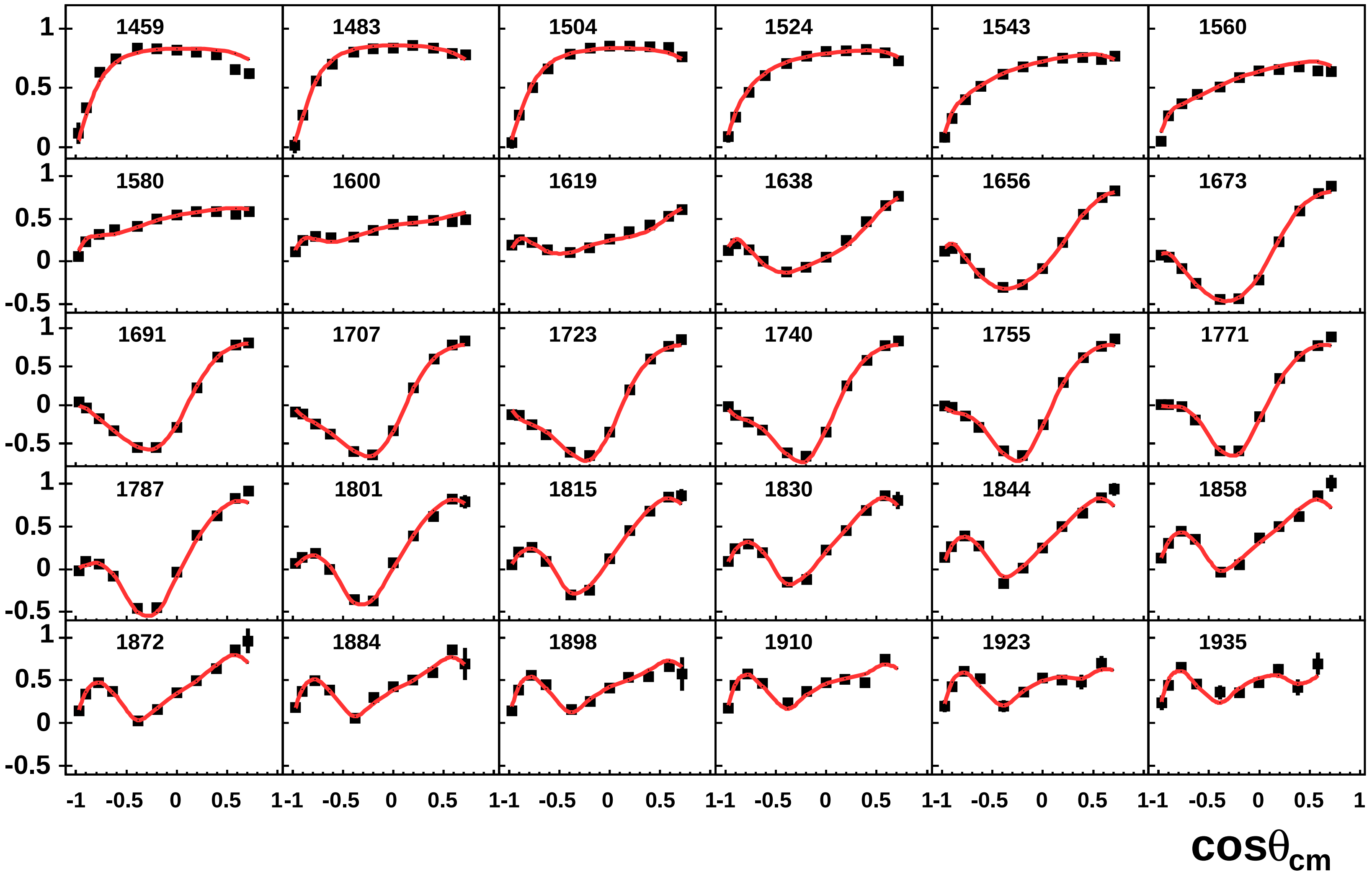

Target asymmetry $T(\gamma p \to \pi^0 p)$

Red curves our fit, Blue curves latest SAID fit

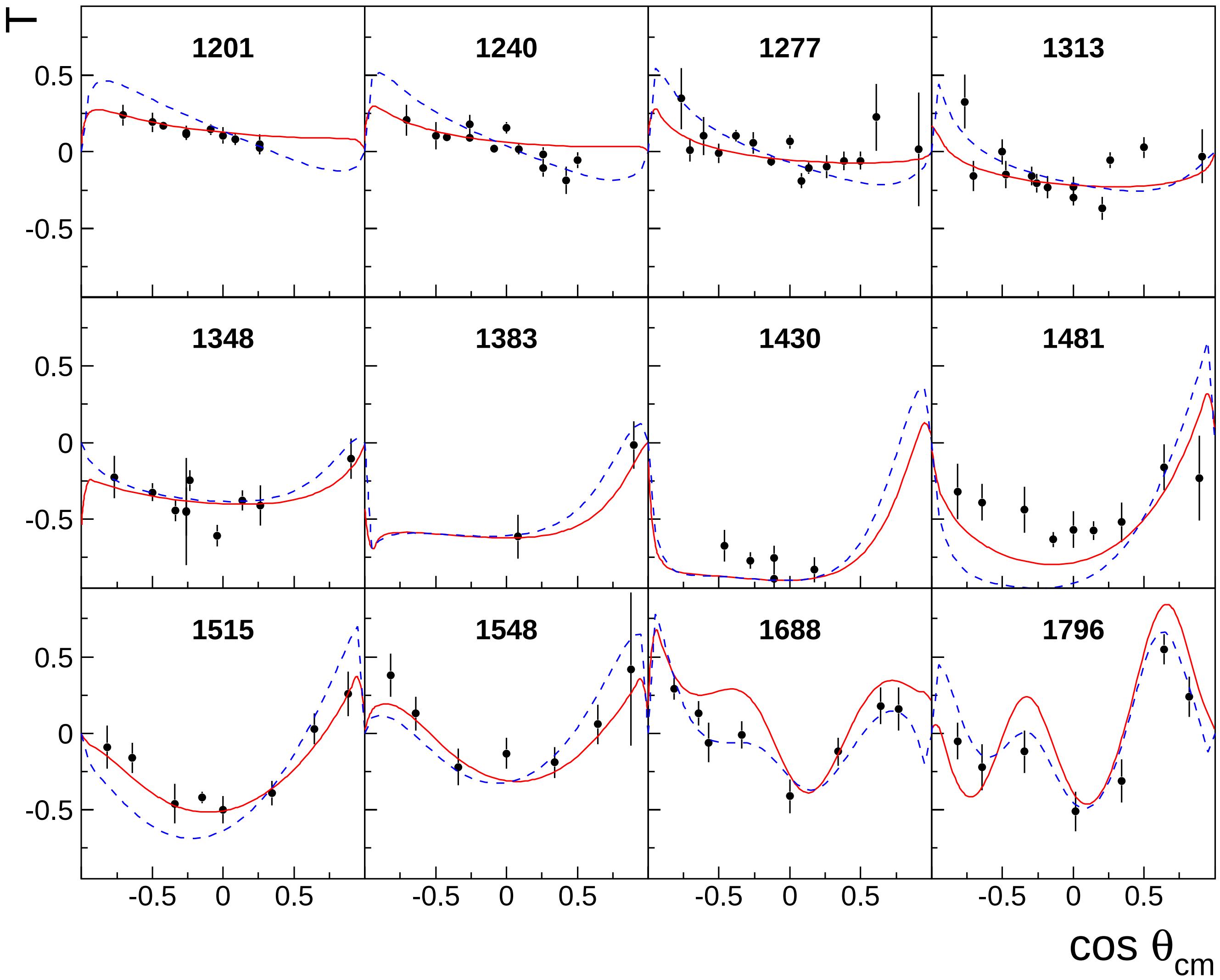

Recoil asymmetry $P(\gamma p \rightarrow \pi^0 p)$

Red curves our fit, Blue curves latest SAID fit

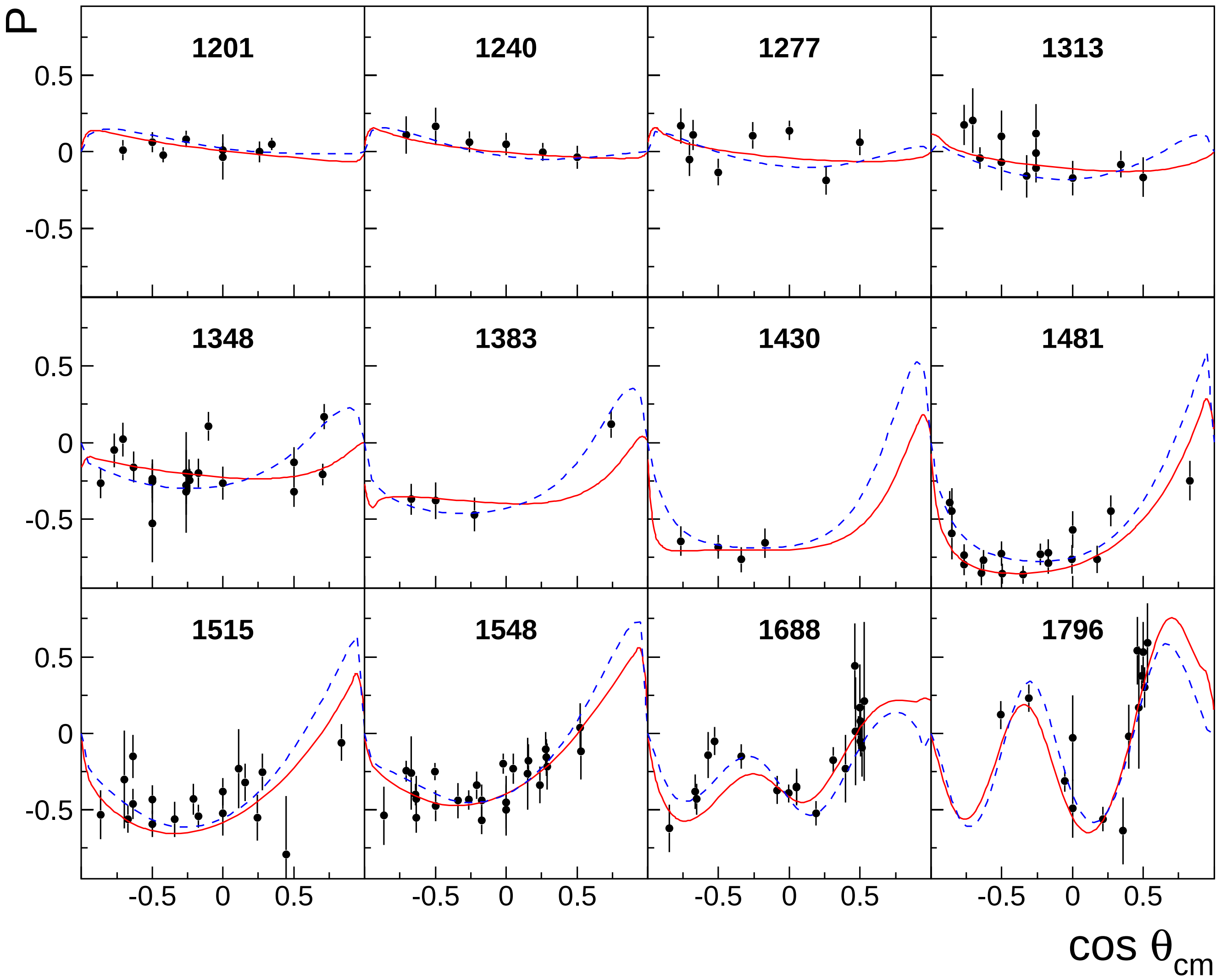

$N\pi \to N\pi$, S_{11} wave (2 pole 4 or 5 channel K-matrix)

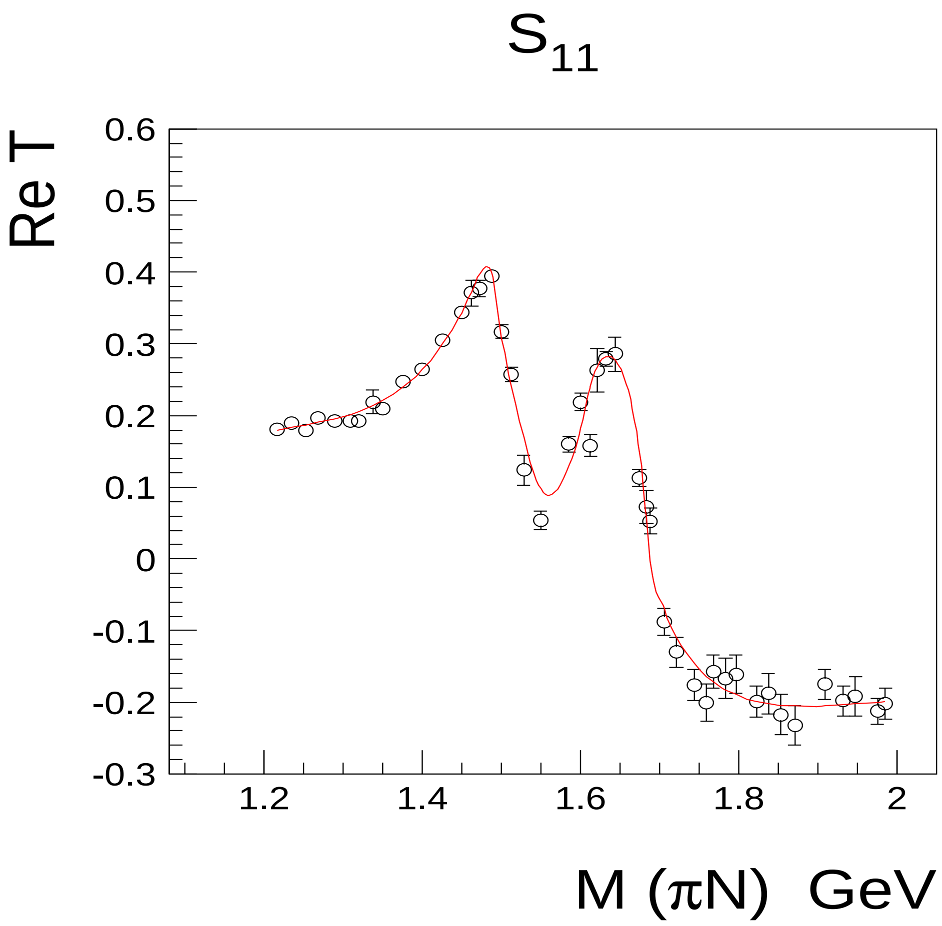

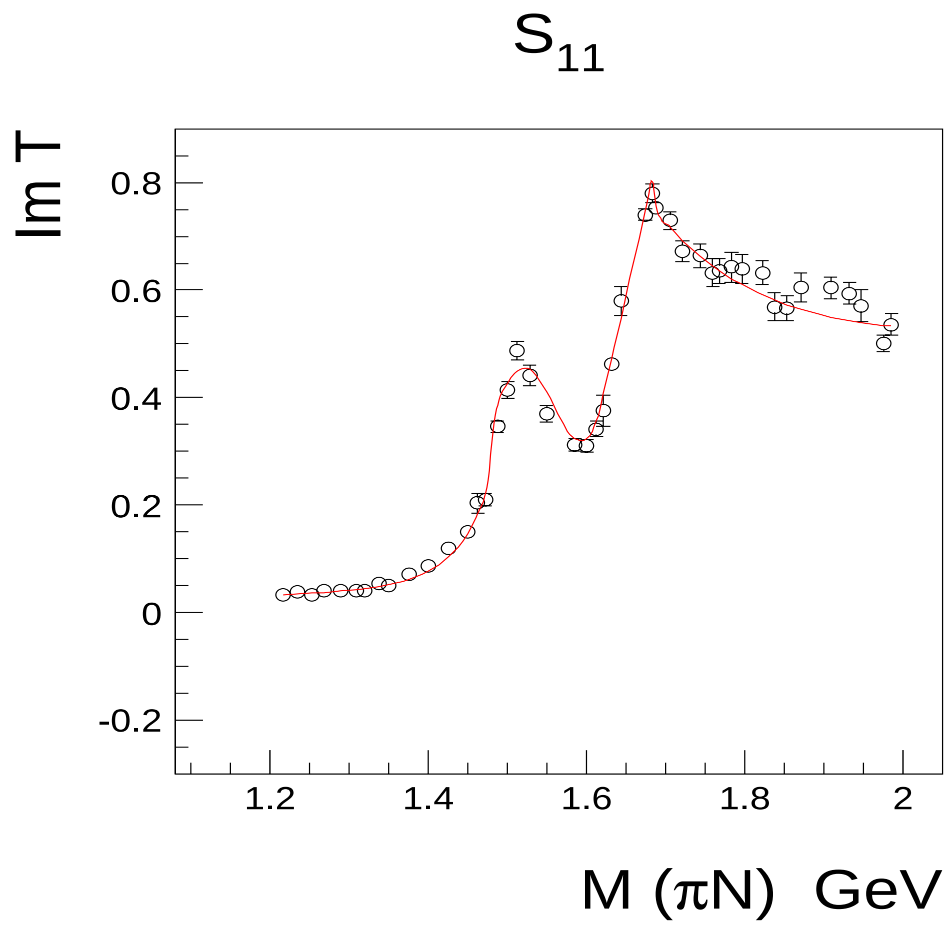

T-matrix poles: $M = 1508^{+10}_{-30}$ **MeV,** $2\ Im = 165 \pm 15$ **MeV;**

$M = 1645 \pm 15$ **MeV,** $2\ Im = 187 \pm 20$ **MeV**

$N\pi \to N\pi$ P_{11} wave (3 pole 4 channel K-matrix)

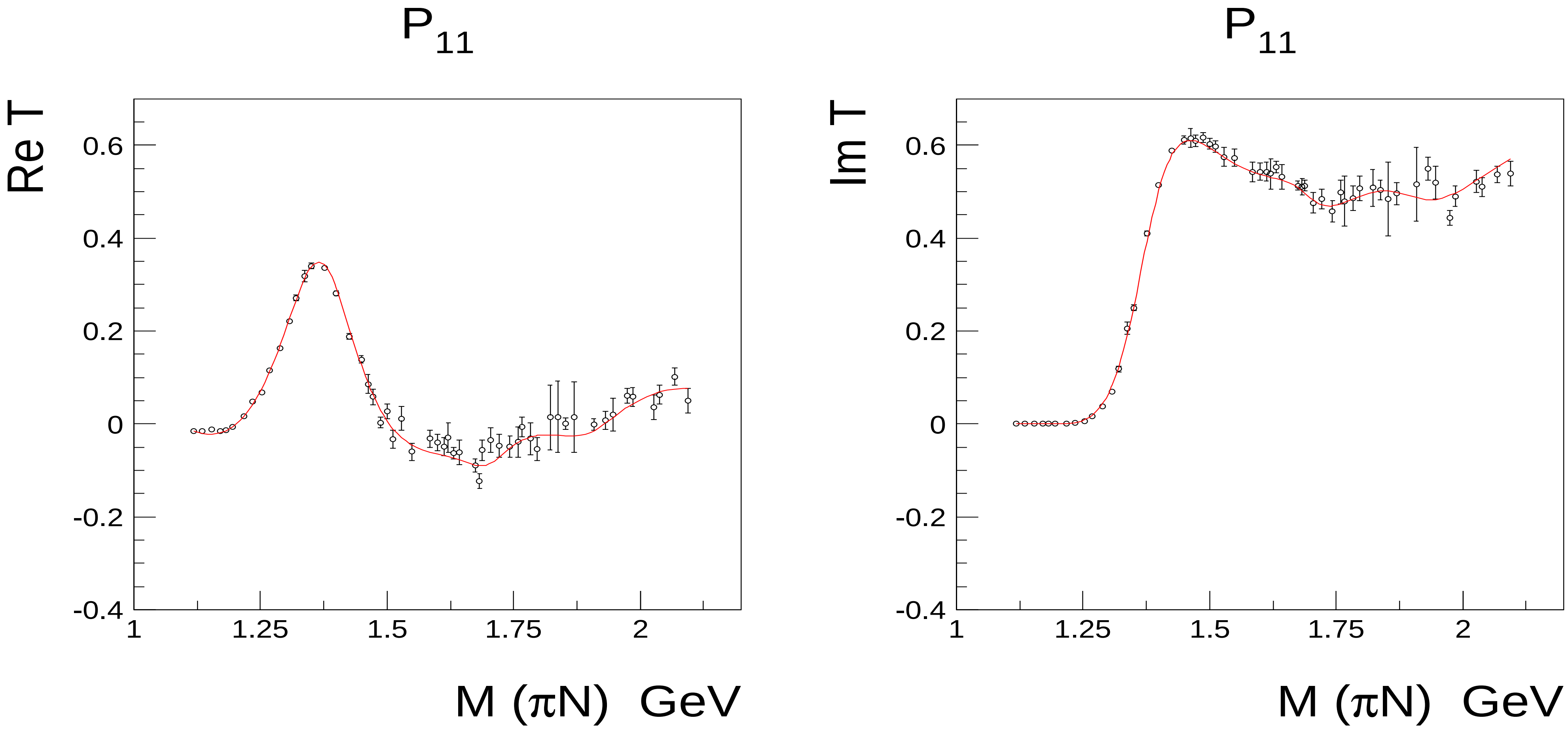

T-matrix poles: $M = 1371 \pm 7$ **MeV,** $2\ Im = 192 \pm 20$ **MeV;**

$M = 1850 \pm 10$ **MeV,** $2\ Im = 150 \pm 20$ **MeV**

$\pi^- p \to n\pi^0\pi^0$ (Crystal Ball) total cross section

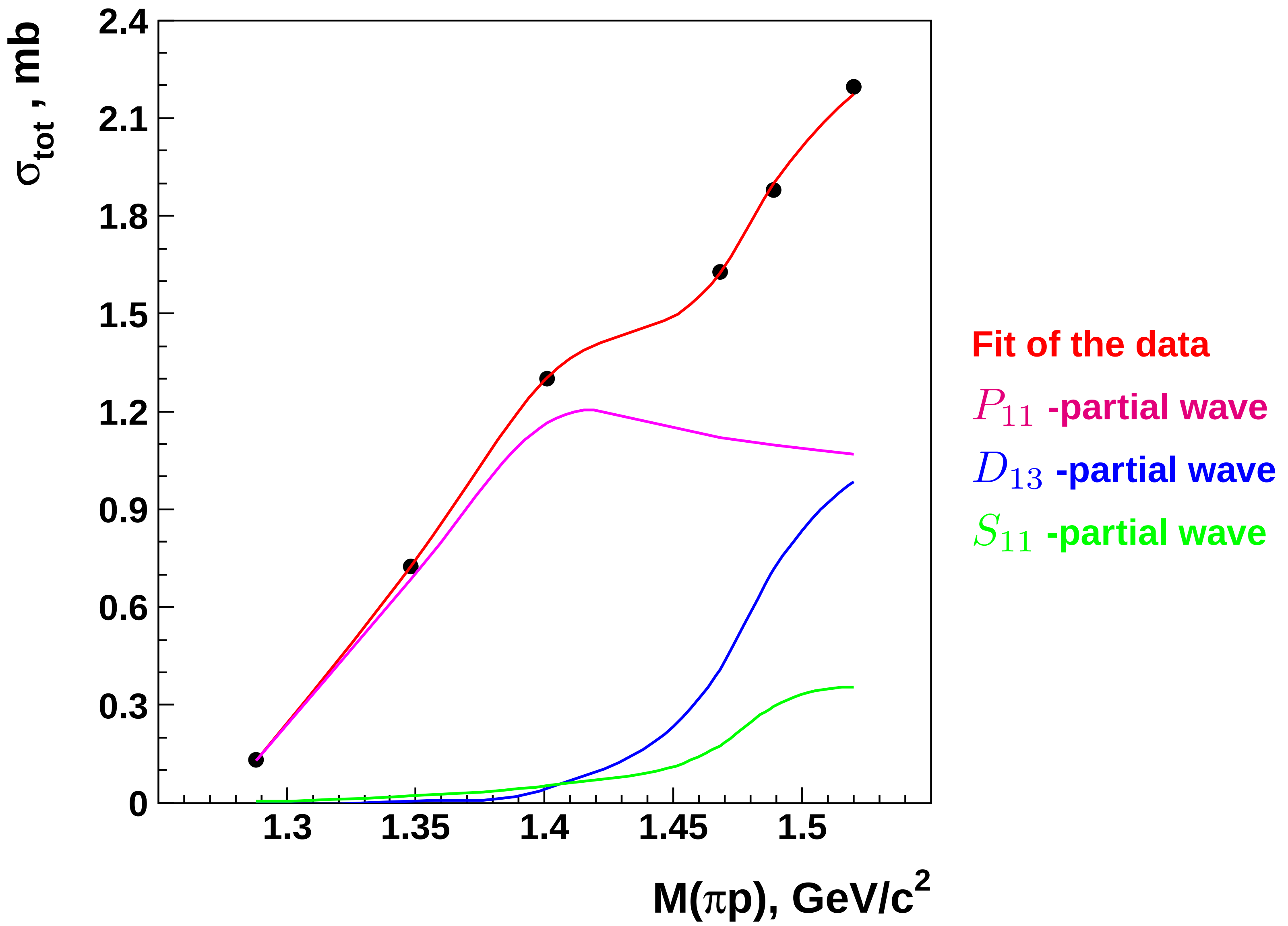

$\pi^- p \to n\pi^0\pi^0$ (Crystal Ball)

Differential cross sections for 472 and 665 MeV/c data.

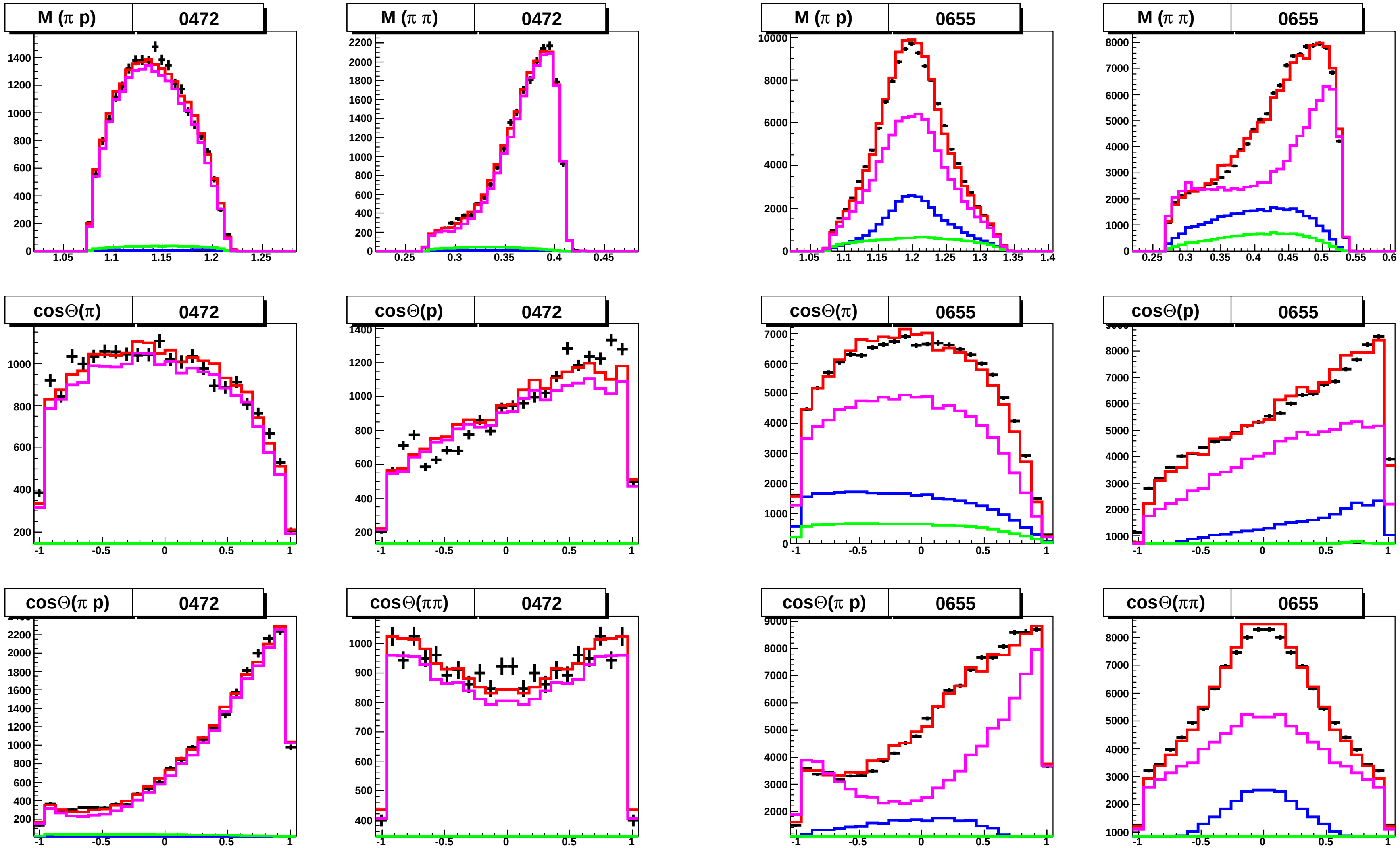

$\gamma p \to p\pi^0\pi^0$ (CB-ELSA) M.Fuchs et al.

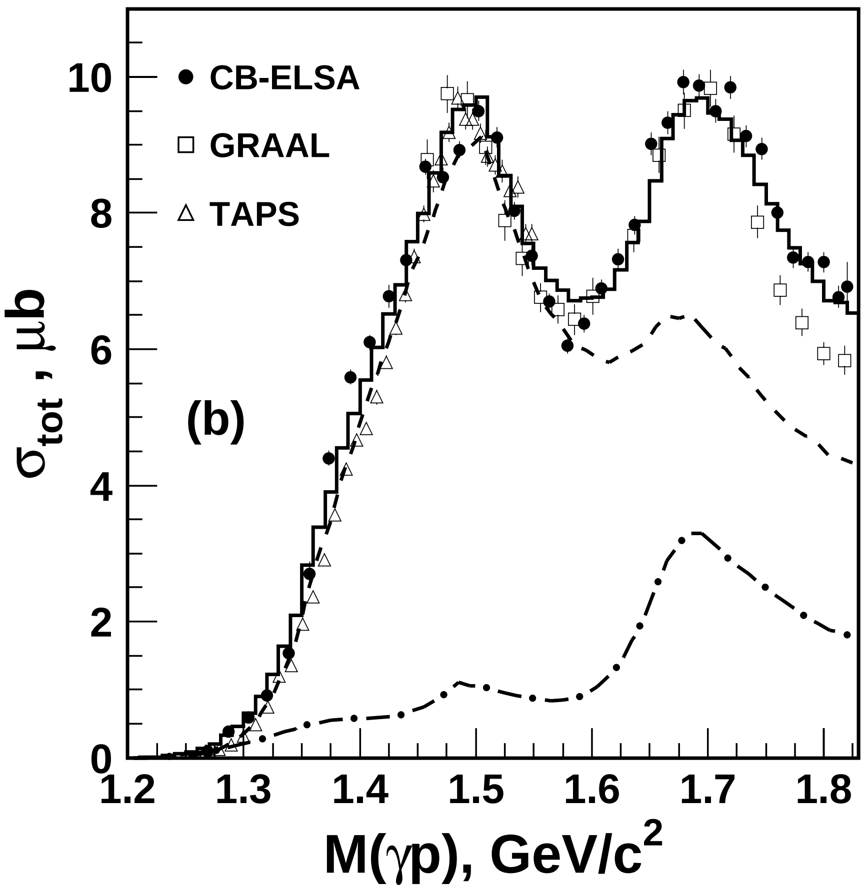

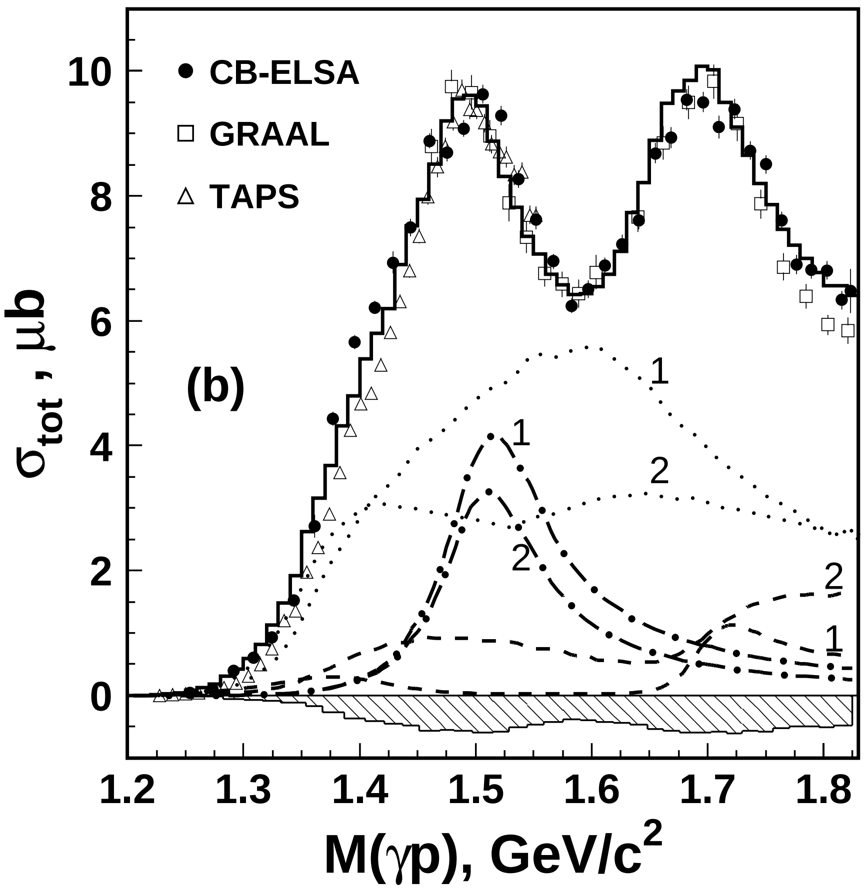

PWA corrected cross section and contributions from $\Delta(1232)\pi$ (dashed) and $N\sigma$ (dashed-dotted) final states.

Contributions from D_{33} (dotted), P_{11} (dashed) and D_{13} (dashed-dotted) partial waves.

Results for our PWA in comparison to $\sigma_{3/2}$, $\sigma_{1/2}$
$\vec{\gamma}\vec{p} \longrightarrow p\pi^0\pi^0$ from Daphne at MAMI

Amplitudes adjusted to our unpolarised data only!:

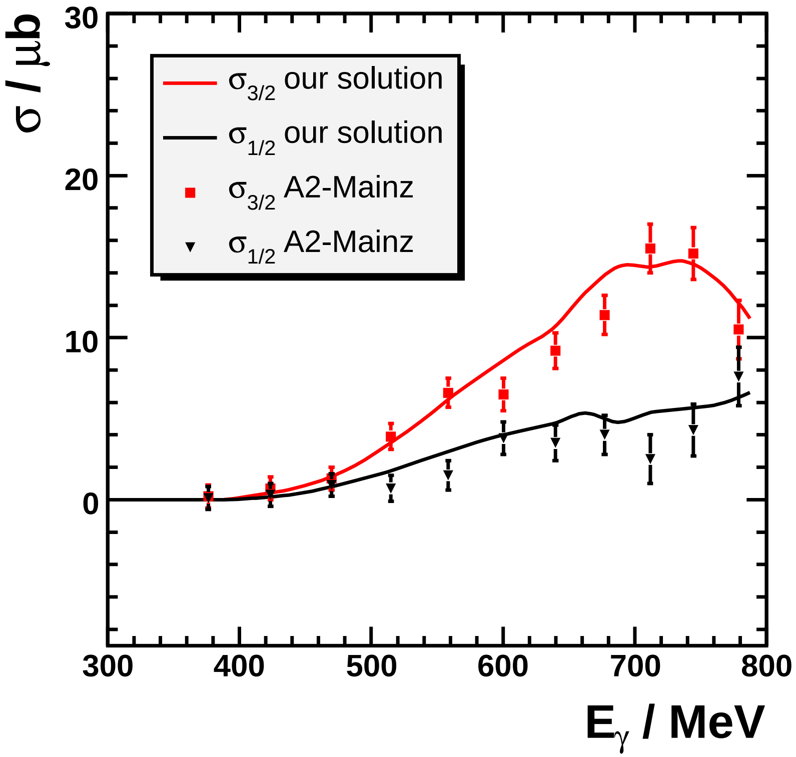

Oset et al.:

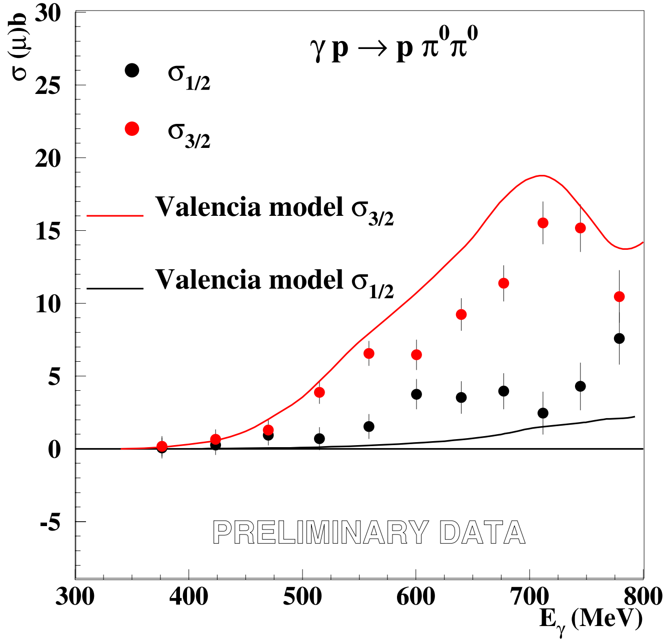

Properties of the low-lying baryons.

	$S_{11}(1535)$	PDG	$S_{11}(1650)$	PDG	$D_{13}(1520)$	PDG
Mass	1508^{+10}_{-30}	1495–1515	1645±15	1640–1680	1509±7	1505–1515
$\Gamma_{\rm tot}$	165±15	90-150	187±20	150-170	113±12	110-120
M_{BW}	1548±15	1520-1555	1655±15	1640–1680	1520±10	1515–1530
Γ^{BW}_{tot}	170±20	100-200	180±20	145-190	125±15	110-135
$A_{1/2}$	86±25	90±30	95±25	53±16	7±15	-(24±9)
$A_{3/2}$					137±12	166±5
$\Gamma_{\rm miss}$	-	< 4 %	-	4–12 %	13±5 %	15–25 %
$\Gamma_{\pi\rm N}$	37±9 %	35–55 %	70±15 %	55–90 %	58±8 %	50–60 %
$\Gamma_{\eta\rm N}$	40±10 %	30–55 %	15±6 %	3–10 %	0.2±0.1 %	0.23±0.04 %
$\rm N\sigma$	-	-	-	< 4 %	< 4 %	< 8 %
$\Gamma_{\rm K\Lambda}$	-		5±5 %	-	-	-
$\Gamma_{\rm K\Sigma}$	-		-		-	
$\Gamma_{\Delta\pi(\rm L<J)}$	-		-		12±4 %	5-12 %
$\Gamma_{\Delta\pi(\rm L>J)}$	23±8 %	< 1 %	10±5 %	< 1 %	14±5 %	10-14 %
$\Gamma_{\rm P_{11}\pi}$	-		-		2±2 %	

Properties of the low-lying baryons.

	$D_{13}(1700)$	PDG	$D_{15}(1675)$	PDG	$P_{13}(1720)$	PDG
Mass	1710$\pm$15	1630-1670	1639$\pm$10	1655–1665	1630$\pm$90	1660–1690
$\Gamma_{\rm tot}$	155$\pm$25	50-150	180$\pm$20	125-155	460$\pm$80	115-275
M$_{BW}$	1740$\pm$20	1650-1750	1678$\pm$15	1670–1685	1790$\pm$100	1700–1750
Γ^{BW}_{tot}	180$\pm$30	50-150	220$\pm$25	140-180	690$\pm$100	150-300
$A_{1/2}$	20$\pm$16	-(18$\pm$13)	25$\pm$10	19$\pm$8	150$\pm$80	18$\pm$30
$A_{3/2}$	75$\pm$30	-(2$\pm$24)	44$\pm$12	-(15$\pm$9)	120$\pm$80	19$\pm$20
$\Gamma_{\rm miss}$	20$\pm$15	$<$35 %	20$\pm$8	1–3 %	-	70–85 %
$\Gamma_{\pi \rm N}$	8$\pm$5 %	5–15 %	30$\pm$8 %	40–50 %	9$\pm$5 %	10–20 %
$\Gamma_{\eta \rm N}$	10$\pm$5 %	0$\pm$1 %	3$\pm$3 %	0–1 %	10$\pm$7 %	4$\pm$1 %
Nσ	18$\pm$12 %		10$\pm$5 %		3$\pm$3 %	
$\Gamma_{\rm K\Lambda}$	1$\pm$1		3$\pm$2 %		12$\pm$9	-
$\Gamma_{\rm K\Sigma}$	$<$1 %		$<$1 %		$<$1 %	
$\Gamma_{\Delta\pi(\rm L<J)}$	10$\pm$5		24$\pm$8		38$\pm$20 %	
$\Gamma_{\Delta\pi(\rm L>J)}$	20$\pm$11 %		$<$3 %		6$\pm$6 %	10-14 %
$\Gamma_{\rm P_{11}\pi}$	14$\pm$8		$<$3 %		–	
$\Gamma_{D_{13}\pi}$	–		4$\pm$4		24$\pm$20 %	

Properties of the low-lying baryons.

	$F_{15}(1680)$	PDG	$S_{31}(1620)$	PDG	$D_{33}(1700)$	PDG
Mass	1674$\pm$5	1665–1675	1615$\pm$25	1580–1620	1610$\pm$35	1620–1700
$\Gamma_{\rm tot}$	95$\pm$10	105-135	180$\pm$35	100-130	320$\pm$60	150-250
	1684$\pm$8	1675–1690	1650$\pm$25	1615–1675	1770$\pm$40	1670–1770
Γ_{tot}^{BW}	105$\pm$8	120-140	250$\pm$60	120-180	630$\pm$150	200-400
$A_{1/2}$	-(12$\pm$8)	-(15$\pm$6)	130$\pm$50	27$\pm$11	125$\pm$30	104$\pm$15
$A_{3/2}$	120$\pm$15	133$\pm$12			150$\pm$60	85$\pm$22
$\Gamma_{\rm miss}$	2$\pm$2%	3–15 %	10$\pm$7%	7–25 %	15$\pm$10 %	30–55 %
$\Gamma_{\pi\rm N}$	72$\pm$15 %	60–70 %	22$\pm$12 %	10–30 %	15$\pm$8 %	10–20 %
$\Gamma_{\eta\rm N}$	$<$ 1 %	0$\pm$1 %	-	-	-	-
$\rm N\sigma$	11$\pm$5%	5–20%	-	-	-	-
$\Gamma_{\rm K\Lambda}$	$<$ 1%		-	-	-	-
$\Gamma_{\rm K\Sigma}$	$<$ 1%					
$\Gamma_{\Delta\pi(\rm L<J)}$	8$\pm$3%	6-14 %	48$\pm$25	30-60%		
					70$\pm$20 %	30–60 %
$\Gamma_{\Delta\pi(\rm L>J)}$	4$\pm$3 %	<2 %				
$\Gamma_{\rm P_{11}\pi}$	-		19$\pm$12 %		$<$5 %	
$\Gamma_{\rm D_{13}\pi}$	-		-		$<$3 %	

Properties of $N(1440)P_{11}$. The left column lists mass, width, partial widths of the Breit-Wigner resonance; the right column pole position and squared couplings to the final state at the pole position.

M	=	1436 ± 15 **MeV**	$\mathbf{M}_{\rm pole}$	=	1371 ± 7 **MeV**
Γ	=	335 ± 40 **MeV**	$\Gamma_{\rm pole}$	=	192 ± 20 **MeV**
$\Gamma_{\pi N}$	=	205 ± 25 **MeV**	$g_{\pi N}$	=	$(0.51 \pm 0.05) \cdot e^{-i\pi \frac{(35\pm5)}{180}}$
$\Gamma_{\sigma N}$	=	71 ± 17 **MeV**	$g_{\sigma N}$	=	$(0.82 \pm 0.16) \cdot e^{-i\pi \frac{(20\pm13)}{180}}$
$\Gamma_{\pi\Delta}$	=	59 ± 15 **MeV**	$g_{\pi\Delta}$	=	$(-0.57 \pm 0.08) \cdot e^{i\pi \frac{(25\pm20)}{180}}$
T-matrix: $A_{1/2} = 0.055 \pm 0.020$ **GeV**			$\phi = (70 \pm 30)^\circ$		

$\gamma p \to \eta p$ from Crystal Barrel at ELSA ($E_\gamma \leq 3.2$ GeV)

Main resonance contributions:

$N(1535)S_{11}$

$N(1650)S_{11}$

$N(1720)P_{13}$

new $N(2070)D_{15}$

Non-resonance contribution: reggezied t-channel $\rho - \omega$ exchange.

No evidence for third $N(1800)S_{11}$

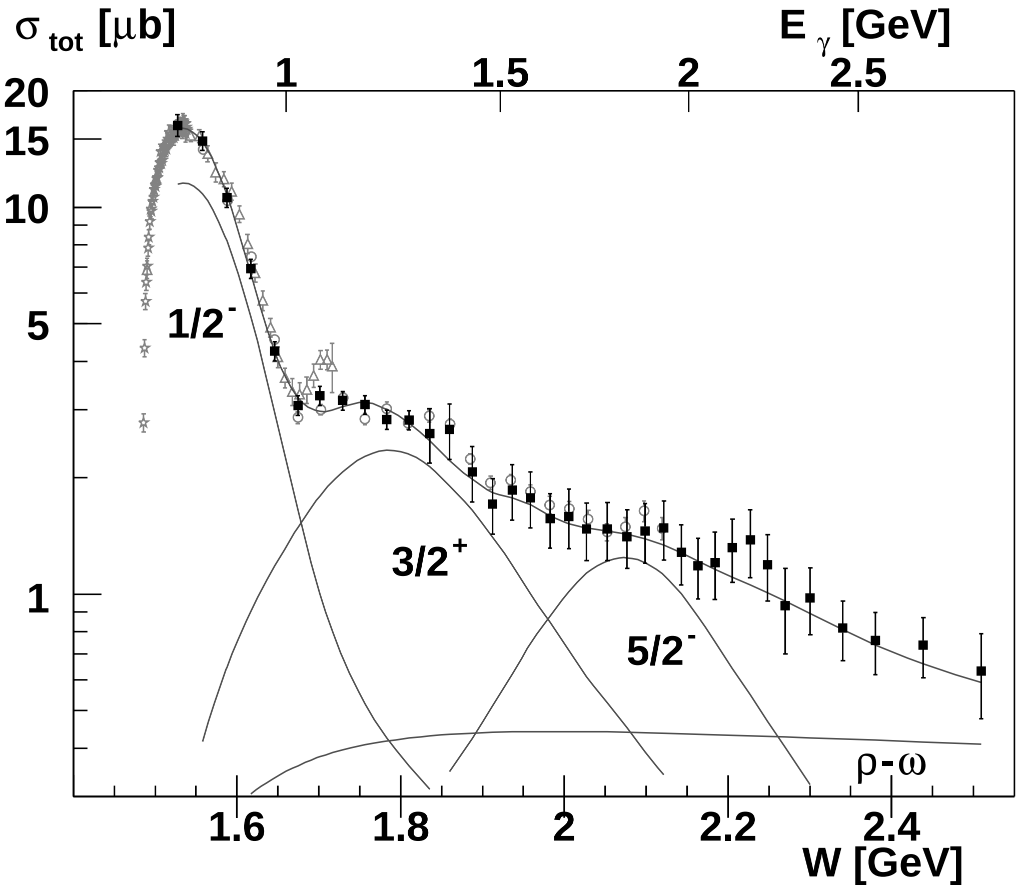

$\gamma p \to \eta p$ from Crystal Barrel at ELSA ($E_\gamma \leq 3.2$ GeV)

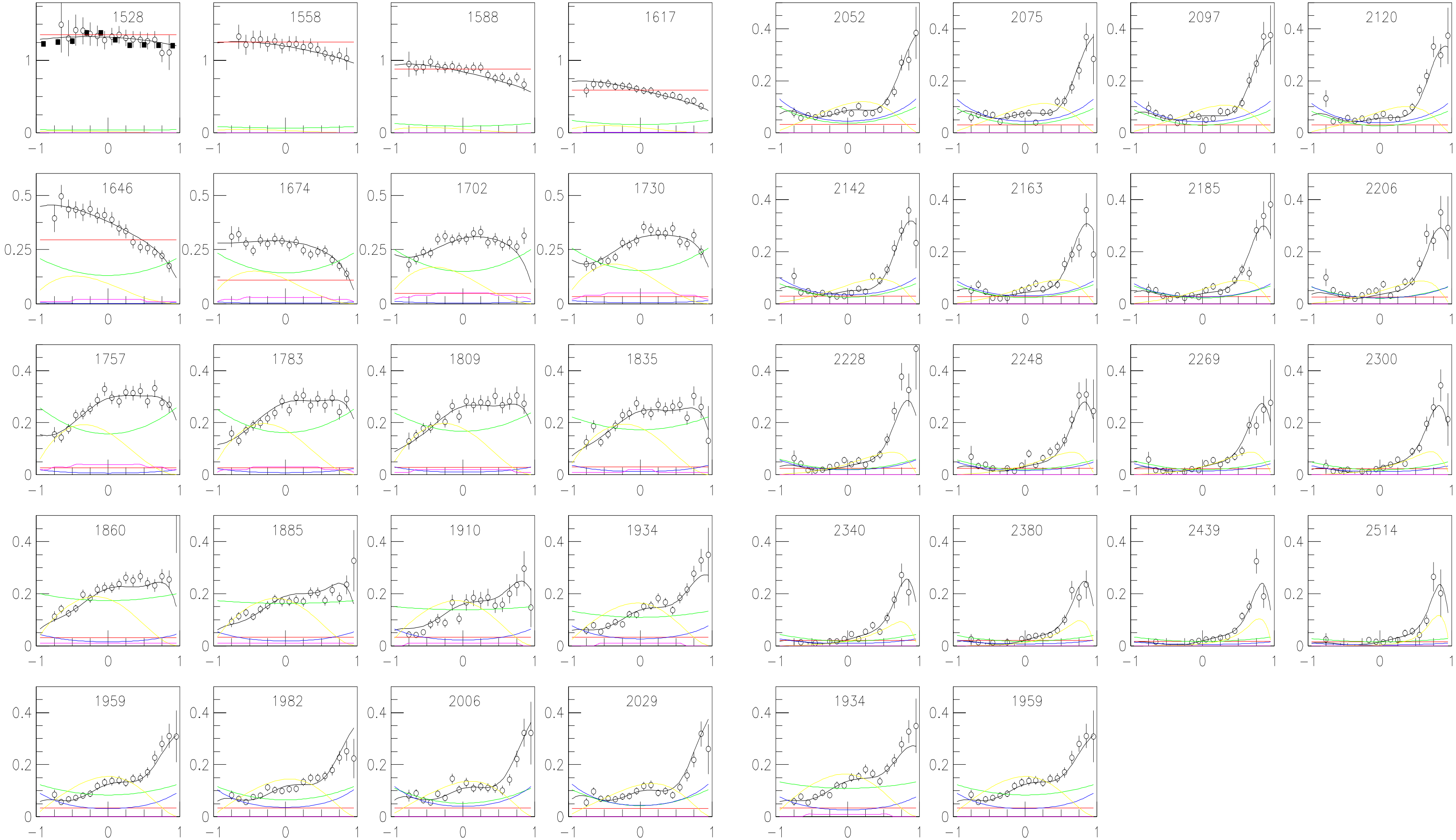

Beam asymmetry $\Sigma(\gamma p \to \eta p)$ from GRAAL 04

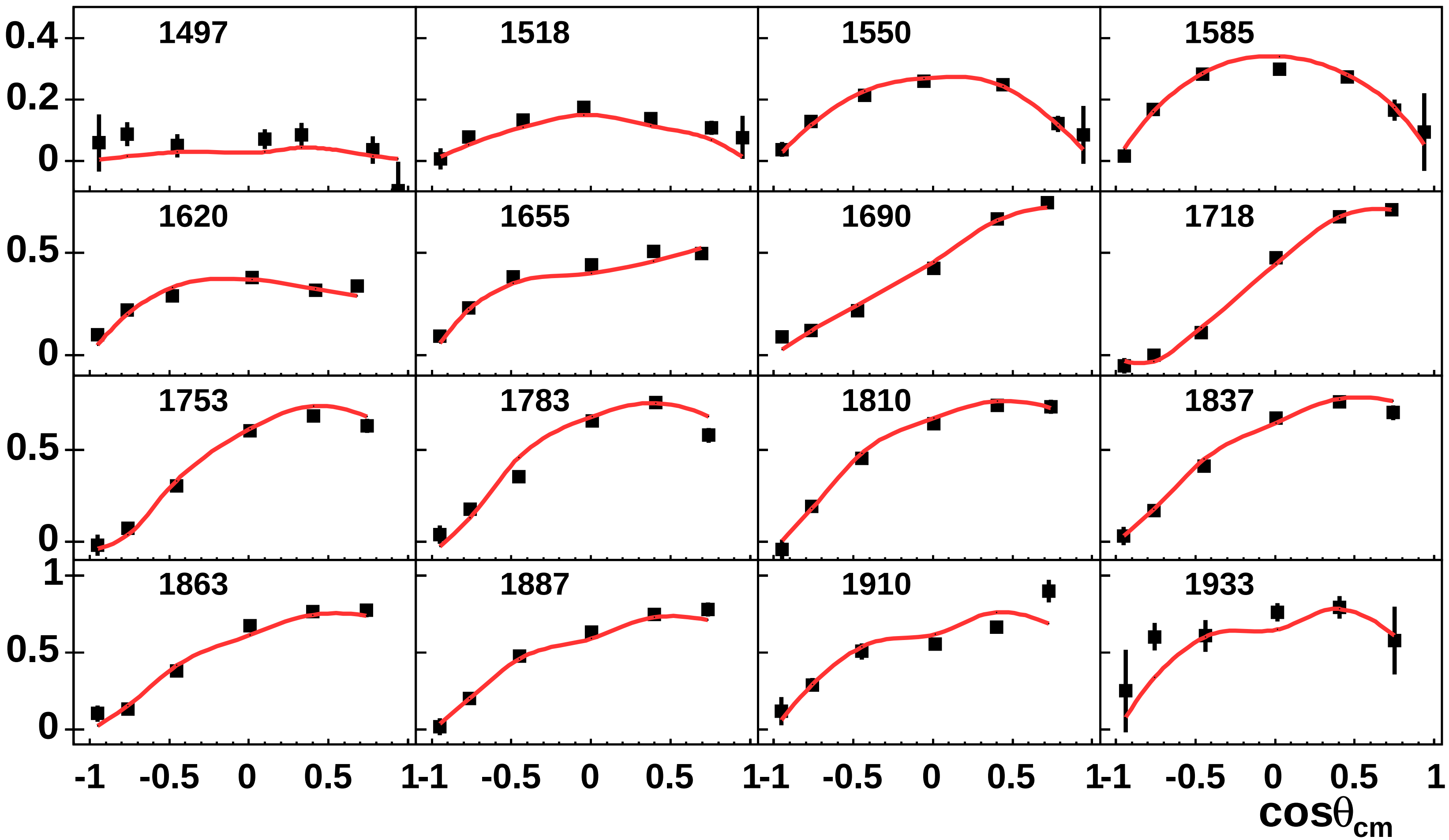

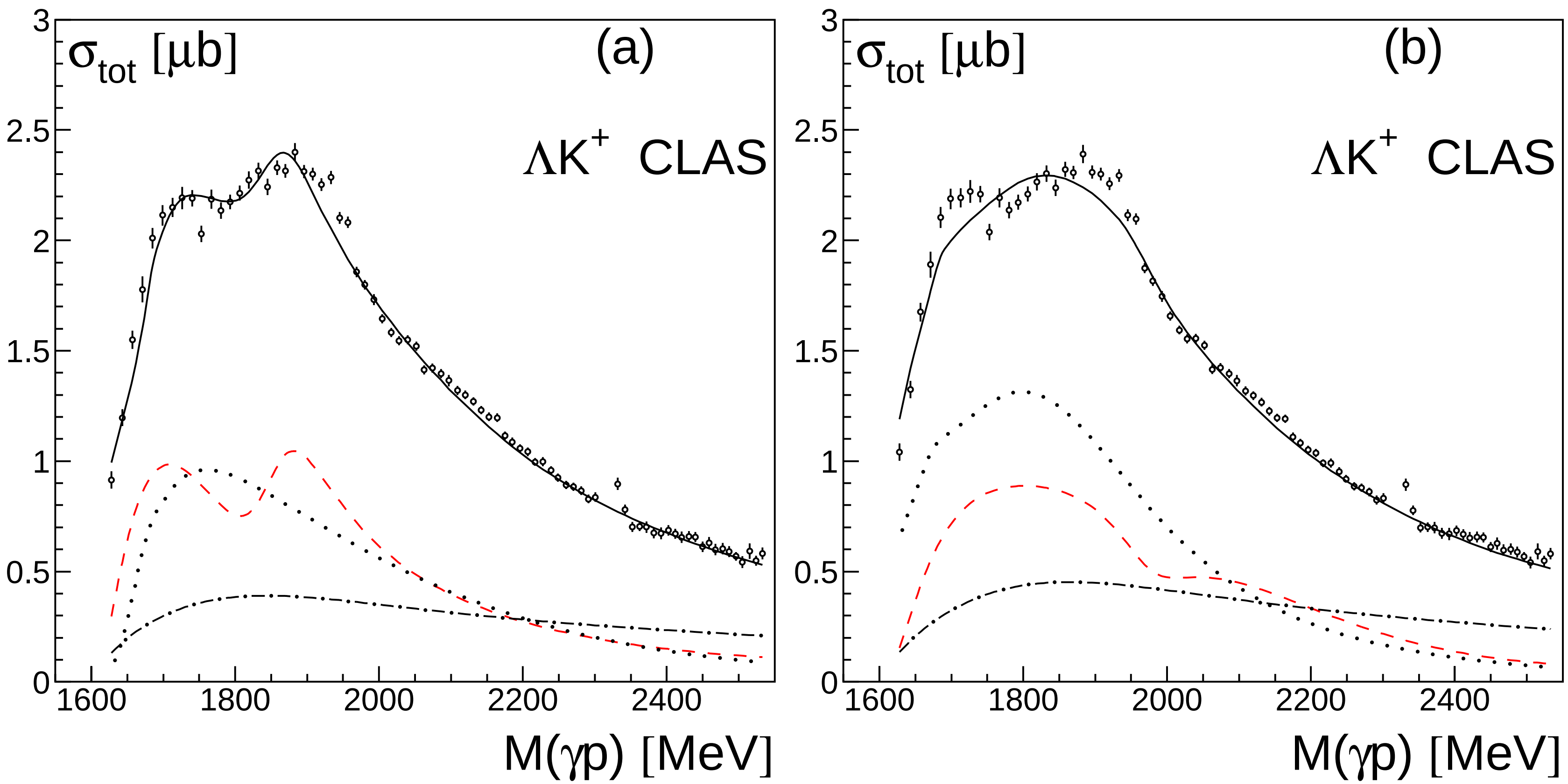

The total cross section for $\gamma p \to \Lambda K^+$ for solution 1 (a) and solution 2 (b). The solid curves are the results of our fits, dashed lines are the P_{13} contribution, dotted lines are the S_{11} contribution and dash-dotted lines are the contribution from K^* exchange.

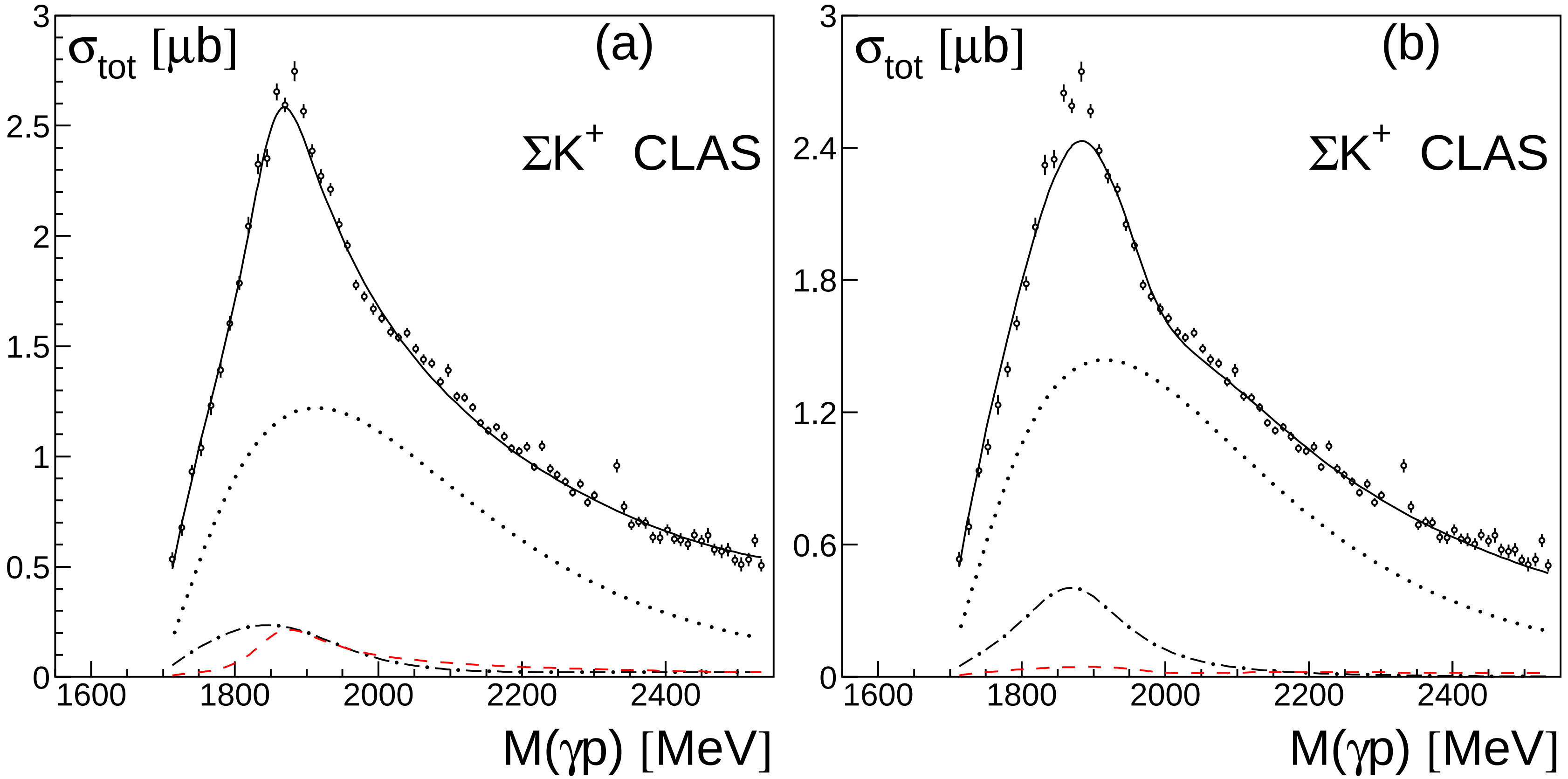

The total cross section for $\gamma p \to \Sigma K$ for solution 1 (a) and solution 2 (b). The solid curves are the results of our fits, dashed lines are the P_{13} contribution, dash-dotted lines are the P_{11} contribution and dotted lines are the contribution from K exchange.

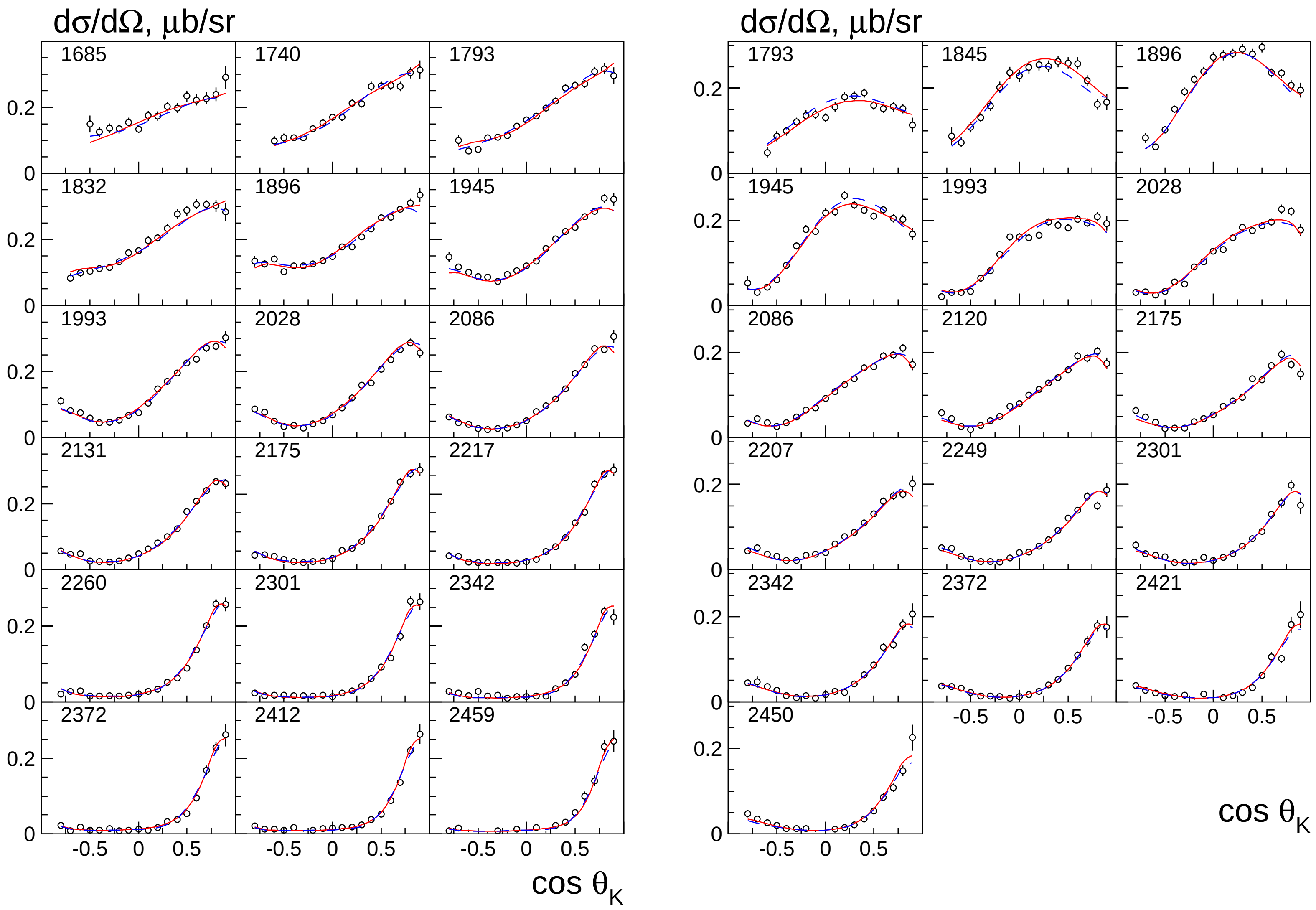

$\gamma p \to \Lambda K^+$ **(left) and** $\gamma p \to \Sigma K$ **(right). Only energy points where** C_x **and** C_z **were measured are shown. The solution 1 (red solid line) and solution 2 (blue dashed line).**

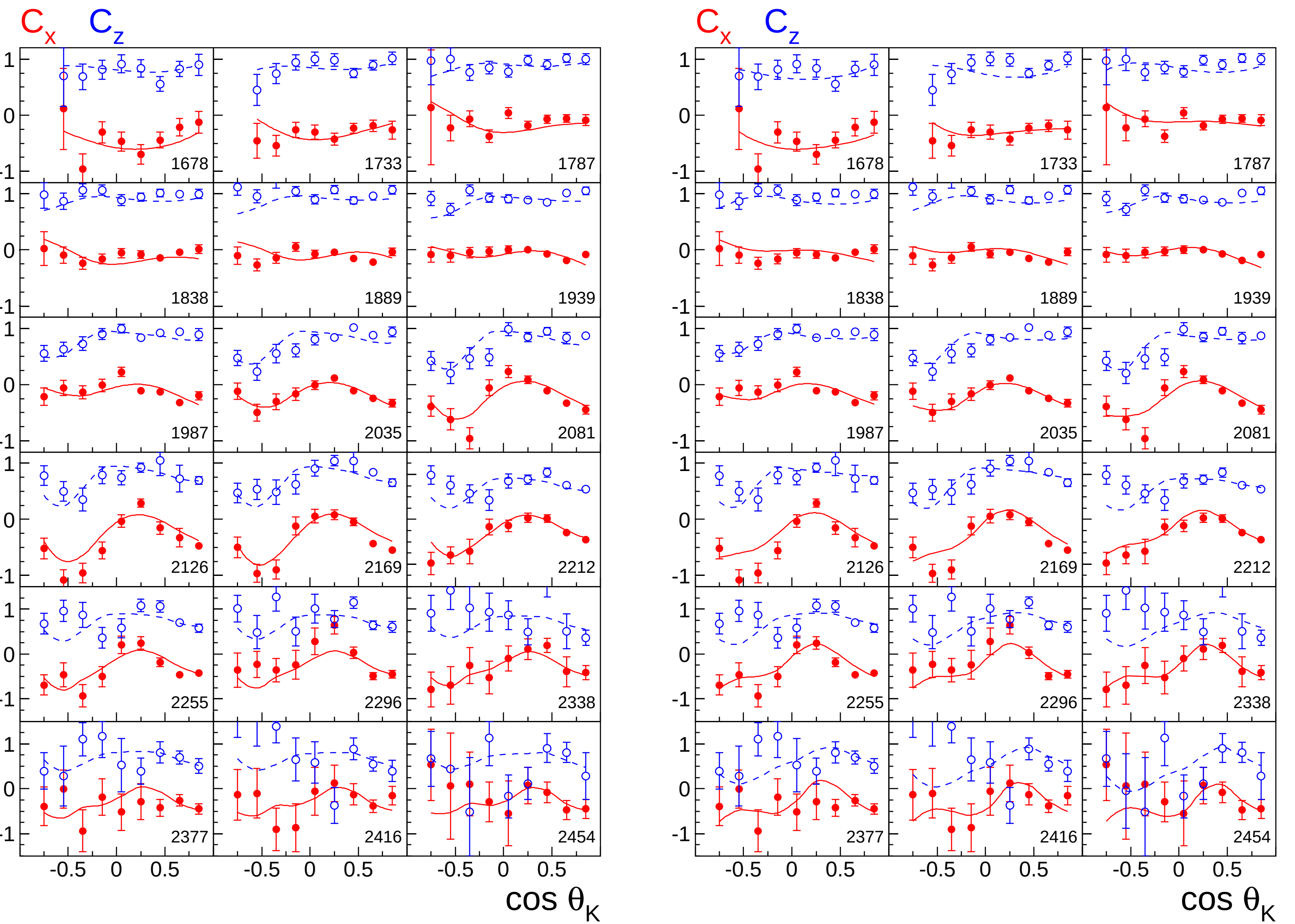

C_x **(black circle) and** C_z **(open circle) for** $\gamma \mathrm{p} \to \Lambda \mathrm{K}^+$**. The solid and dashed curves are results of our fit obtained with solution 1 (left) and solution 2 (right) for** C_x **and** C_z**.**

Properties of the two lowest P_{13} states for two solutions:

	Solution 1		Solution 2	
M_{pole}	1640 ± 80	1870 ± 15	1630 ± 60	1960 ± 15
Γ_{tot}^{pole}	480 ± 60	170 ± 30	440 ± 60	195 ± 25
M_{BW}	1800 ± 100	1885 ± 15	1780 ± 80	1975 ± 15
Γ_{tot}^{BW}	700 ± 100	180 ± 25	680 ± 80	200 ± 25
$A_{1/2}$	140 ± 80	$-(15 \pm 15)$	160 ± 40	$-(18 \pm 8)$
$\varphi_{1/2}$	$-(10 \pm 15)^\circ$	–	$(10 \pm 15)^\circ$	$(40 \pm 15)^\circ$
$A_{3/2}$	150 ± 80	$-(40 \pm 15)$	70 ± 30	$-(35 \pm 12)$
$\varphi_{3/2}$	$-(40 \pm 30)^\circ$	$-(20 \pm 15)^\circ$	$(0 \pm 20)^\circ$	$-(40 \pm 15)^\circ$
$\mathrm{Br}_{N\pi}$	8 ± 4	5 ± 3	11 ± 4	6 ± 3
$\mathrm{Br}_{N\eta}$	13 ± 4	21 ± 8	5 ± 2	15 ± 3
$\mathrm{Br}_{\Delta\pi(P)}$	48 ± 10	3 ± 2	28 ± 6	7 ± 2
$\mathrm{Br}_{\Delta\pi(F)}$	2 ± 2	4 ± 3	11 ± 4	21 ± 5
$\mathrm{Br}_{K\Lambda}$	15 ± 6	10 ± 5	5 ± 2	12 ± 3
$\mathrm{Br}_{K\Sigma}$	< 1	20 ± 8	< 1	8 ± 2
$\mathrm{Br}_{D_{13}\pi}$	10 ± 6	8 ± 3	38 ± 6	5 ± 3
$\mathrm{Br}_{N\sigma}$	4 ± 2	30 ± 12	2 ± 2	26 ± 8

$\sigma_{tot}(\gamma p \to K^0\Sigma^+)$ from CB-ELSA

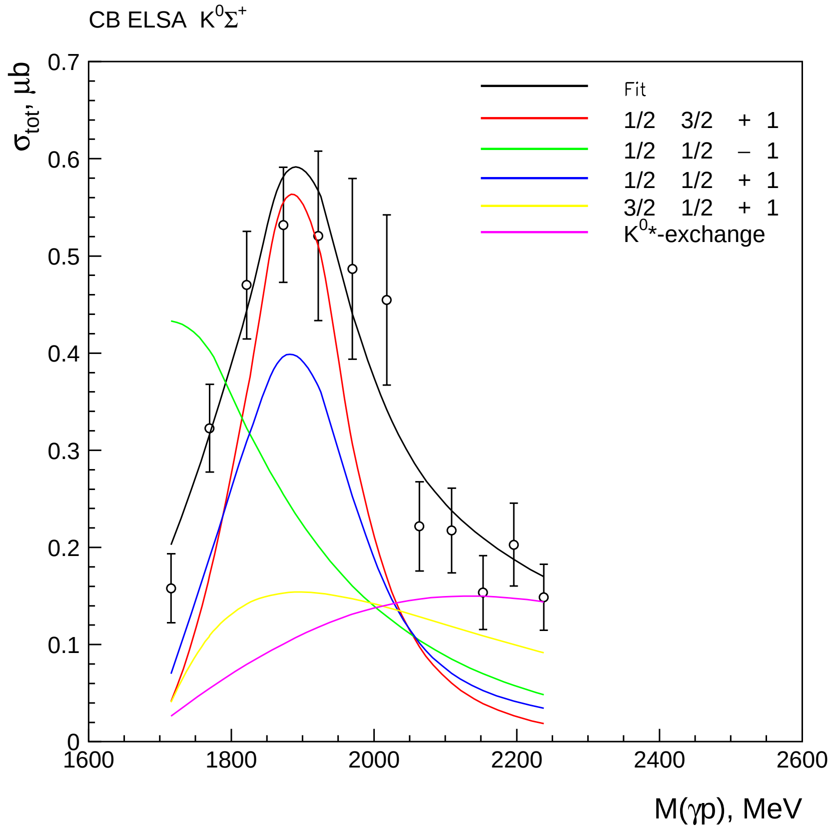

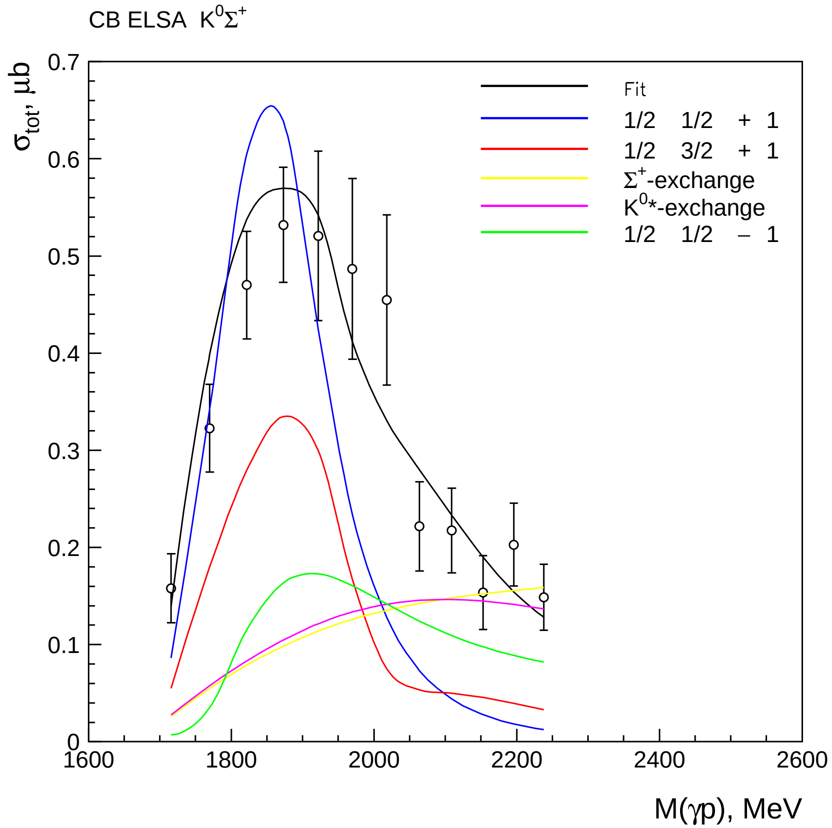

Red line – $P_{13}(1900)$

Blue line – $P_{11}(1860)$

$\gamma p \to p\pi^0\eta$ (CB-ELSA) I.Horn et al.

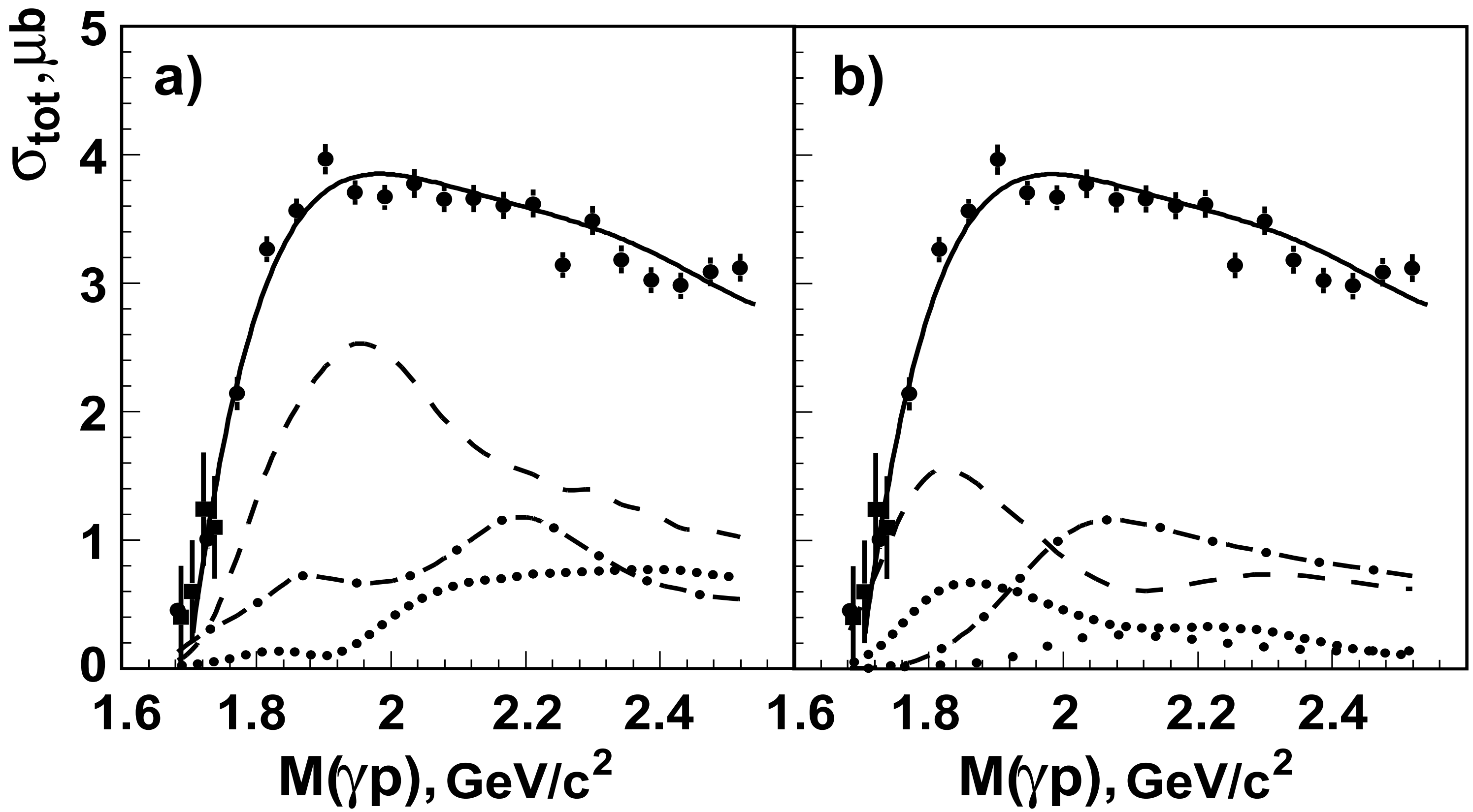

Left panel : contributions from $\Delta(1232)\eta$ (dashed), $S_{11}(1535)\pi$ (dashed-dotted) and $N\,a_0(980)$ final states.

Right panel: D_{33} partial wave (dashed), P_{33} partial wave (dashed-dotted), $D_{33} \to \Delta(1232)\eta$ (dotted) and $D_{33} \to N\,a_0(980)$ (wide dotted).

The $\gamma p \to \pi^0 \eta p$ differential cross section for the total energy region.

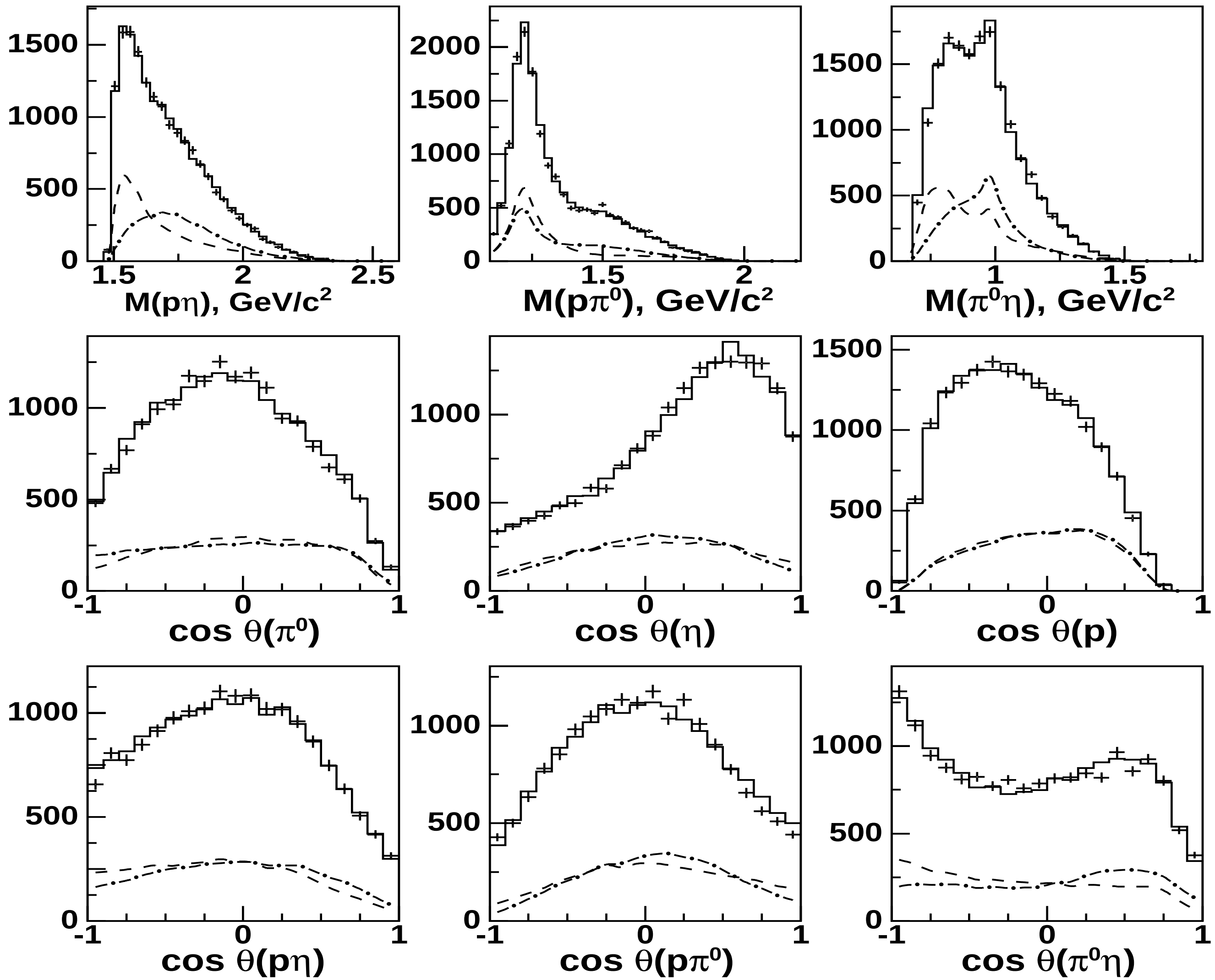

$N\pi \to N\pi$ D_{33} wave (3 pole 5 channel K-matrix)

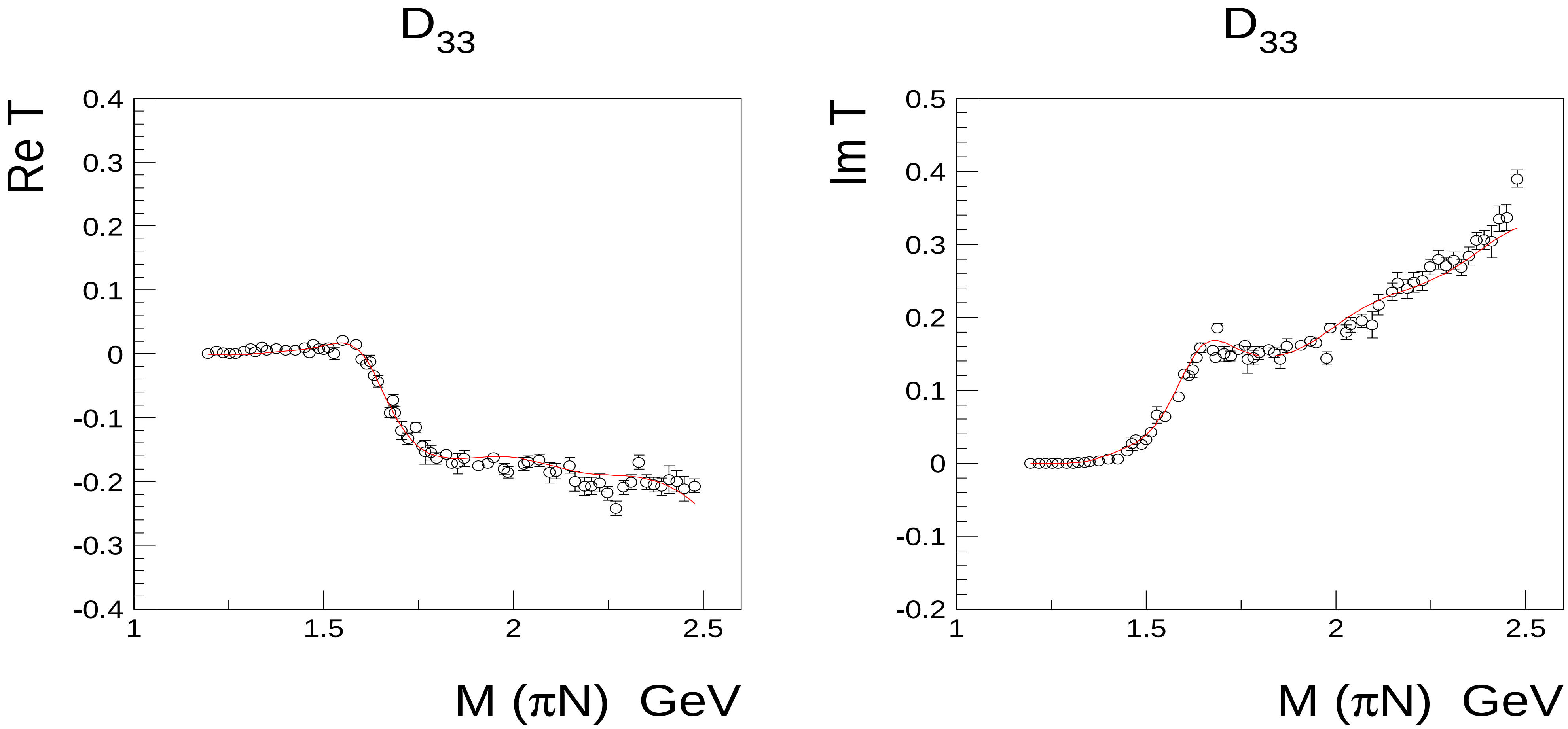

D_{33}**-wave:** πN, $\Delta(1232)\pi$ **(**S**- and** D**-waves)),** $\Delta(1232)\eta$, $S_{11}(1535)\pi$

Properties of the $\Delta(1920)P_{33}$ and $\Delta(1940)D_{33}$ resonances.

	M_{pole}	Γ_{pole}	M_{BW}	Γ_{tot}^{BW}
$\Delta(1920)P_{33}$	1980^{+25}_{-45}	350^{+35}_{-55}	1990 ± 35	375 ± 50
$\Delta(1940)D_{33}$	1985 ± 30	390 ± 50	1990 ± 40	410 ± 70

	$\mathrm{Br}_{N\pi}$	$\mathrm{Br}_{\Delta\eta}$	$\mathrm{Br}_{N(1535)\pi}$	$\mathrm{Br}_{Na_0(980)}$
$\Delta(1920)P_{33}$	15 ± 8	18 ± 8	7 ± 4	4 ± 2
$\Delta(1940)D_{33}$	9 ± 4	5 ± 2	2 ± 1	2 ± 1

Parity doublets and chiral multiplets of N and Δ resonances of high mass

Glozman suggested a restoration of chiral symmetry in high-mass excitations. Parity doublets must not interact by pion emission or absorption and have a small coupling to πN.

J=$\frac{1}{2}$	N$_{1/2+}(2100)^a$	*	N$_{1/2-}(2090)^a$	*	$\Delta_{1/2+}(1910)$	****	$\Delta_{1/2-}(1900)^a$	**
J=$\frac{3}{2}$	N$_{3/2+}(1900)^a$	**	N$_{3/2-}(2080)^a$	**	$\Delta_{3/2+}(1920)^a$	***	$\Delta_{3/2-}(1940)^a$	*
J=$\frac{5}{2}$	N$_{5/2+}(2000)^a$	**	N$_{5/2-}(2200)^a$	**	$\Delta_{5/2+}(1905)$	****	$\Delta_{5/2-}(1930)^a$	***
J=$\frac{7}{2}$	N$_{7/2+}(1990)^a$	**	N$_{7/2-}(2190)$	****	$\Delta_{7/2+}(1950)$	****	$\Delta_{7/2-}(2200)^a$	*
J=$\frac{9}{2}$	N$_{9/2+}(2220)$	****	N$_{9/2-}(2250)$	****	$\Delta_{9/2+}(2300)$	**	$\Delta_{9/2-}(2400)^a$	**

Problem: the absence of a near-by parity partner of $\Delta(1950)F_{37}$ and partners of $\Delta(2420)H_{3\,11}$ and $\Delta(2950)K_{3\,11}$. However these states can be still undetected.

Holographic QCD (AdS/QCD)

Soft-wall model prediction: $M^2_{N,L} = 4\lambda^2\left(N+L+\frac{3}{2}\right)$

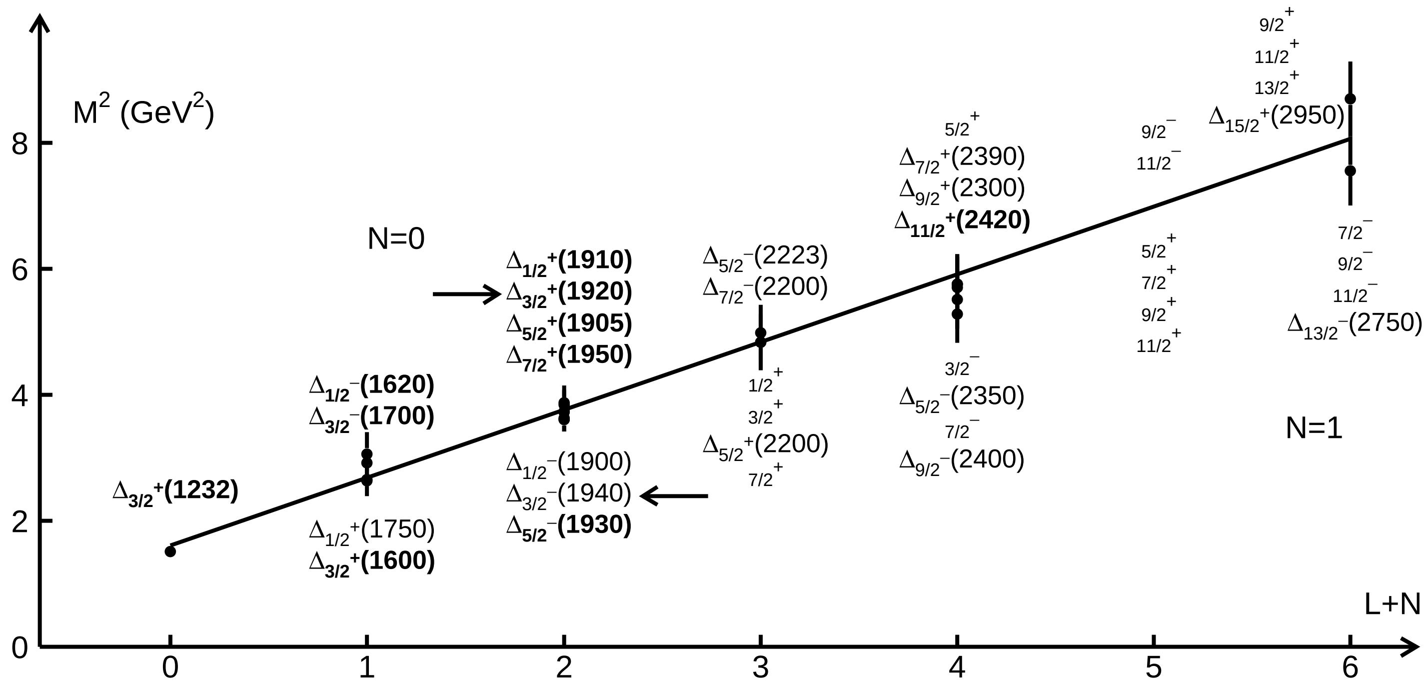

$$M^2_{N,L} = 4\lambda^2\left(N+L+\frac{3}{2}\right) - 2\left(M^2_\Delta - M^2_N\right)\kappa_{gd}$$

κ_{gd} **is the fraction of most attractive color-antitriplet isosinglet diquark.**

κ_{gd}**=0 for** Δ **and N(S=3/2) states,** $\frac{1}{2}$ **for** $S=1/2\ (70SU_6)$ **and** $\frac{1}{4}$ **for** $S=1/2\ (56SU_6)$**.**

Hilmar Forkel and Eberhard Klempt, hep-ph:0810.2959v1

L,S,N	κ_{gd}	Resonance					Pred.
0,$\frac{1}{2}$,0	$\frac{1}{2}$	$N(940)$				**input:**	**0.94**
0,$\frac{3}{2}$,0	**0**	$\Delta(1232)$					**1.27**
0,$\frac{1}{2}$,1	$\frac{1}{2}$	$N(1440)$					**1.40**
1,$\frac{1}{2}$,0	$\frac{1}{4}$	$N(1535)$	$N(1520)$				**1.53**
1,$\frac{3}{2}$,0	**0**	$N(1650)$	$N(1700)$	$N(1675)$			**1.64**
1,$\frac{1}{2}$,0	**0**	$\Delta(1620)$	$\Delta(1700)$		L,S,N**=0,$\frac{3}{2}$,1:**	$\Delta(1600)$	**1.64**
2,$\frac{1}{2}$,0	$\frac{1}{2}$	$N(1720)$	$N(1680)$		L,S,N**=0,$\frac{1}{2}$,2:**	$N(1710)$	**1.72**
1,$\frac{3}{2}$,1	**0**	$\Delta(1900)$	$\Delta(1940)$	$\Delta(1930)$			**1.92**
2,$\frac{3}{2}$,0	**0**	$\Delta(1910)$	$\Delta(1920)$	$\Delta(1905)$	$\Delta(1950)$		**1.92**
2,$\frac{3}{2}$,0	**0**	$N(1880)$	$N(1900)$	$N(1990)$	$N(2000)$		**1.92**
0,$\frac{1}{2}$,3	$\frac{1}{2}$	$N(2100)$					**2.03**
3,$\frac{1}{2}$,0	$\frac{1}{4}$	$N(2070)$	$N(2190)$	L,S,N**=1,$\frac{1}{2}$,2:**	$N(2080)$	$N(2090)$	**2.12**
3,$\frac{3}{2}$,0	**0**	$N(2200)$	$N(2250)$	L,S,N**=1,$\frac{1}{2}$,2:**	$\Delta(2223)$	$\Delta(2200)$	**2.20**
4,$\frac{1}{2}$,0	$\frac{1}{2}$	$N(2220)$					**2.27**
4,$\frac{3}{2}$,0	**0**	$\Delta(2390)$	$\Delta(2300)$	$\Delta(2420)$	$\vert L,N$**=3,1:**	$\Delta(2400)$ $\Delta(2350)$	**2.43**
5,$\frac{1}{2}$,0	$\frac{1}{4}$	$N(2600)$					**2.57**

η-photoproduction at the neutron - CB-ELSA/TAPS data -

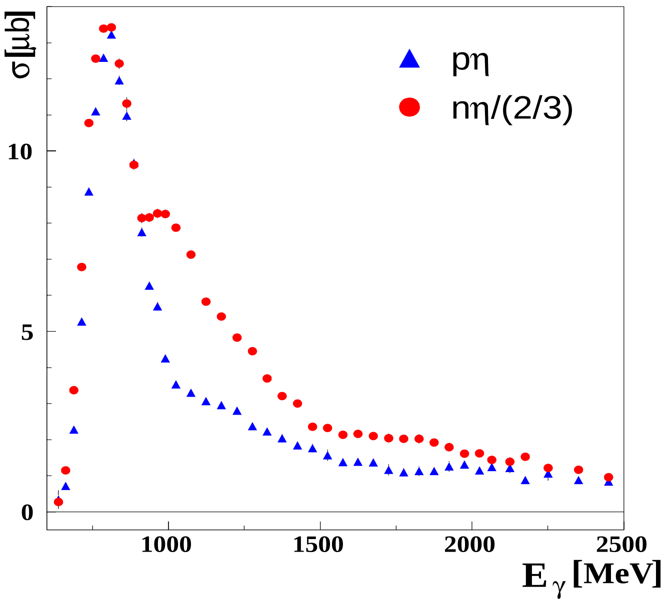

Investigation of $\gamma d \rightarrow n\eta\ (p);\ \eta \rightarrow 3\pi^0$

$\leftrightarrow$ also CB-ELSA/TAPS data shows an enhancement around 1670 MeV (preliminary)

σ_n/σ_p data in comparison to MAID (—) prediction $\Rightarrow$

$\leftrightarrow$ effect of the $D_{15}(1675)$

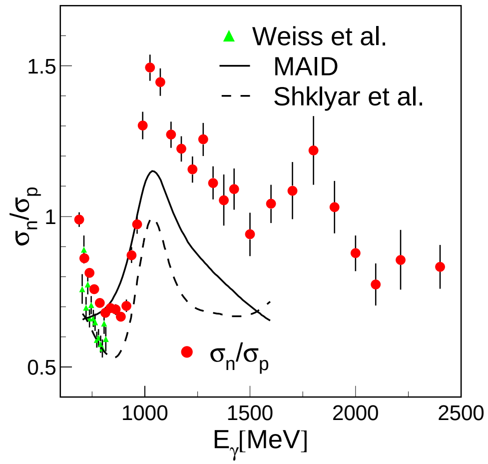

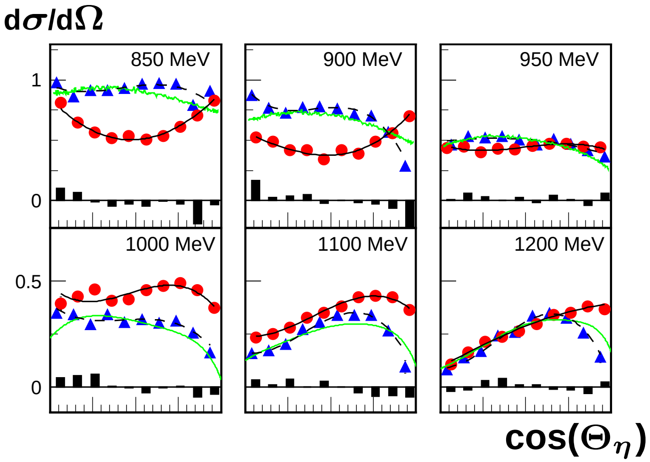

$\leftrightarrow$ something quite interesting going on

- role of the $D_{15}(1675)$?
- narrow $P_{11}(1670)$?
- explainable by S_{11}-states + $P_{11}(1710)$?
- interference of $S_{11}(1535)/S_{11}(1650)$?

$\leftrightarrow$ additional observables needed

Three different class of solutions are found:

1. **solutions with strong interference in S_{11} wave;**
2. **solutions with $N(1710)P_{11}$ resonance;**
3. **solutions with narrow state in the mass region 1665 MeV.**

Observable	$N_{\rm data}$	$\frac{\chi^2}{N_{\rm data}}$	$\frac{\chi^2}{N_{\rm data}}$	$\frac{\chi^2}{N_{\rm data}}$	Ref.
		Sol. 1	**Sol. 2**	**Sol. 3**	
$\sigma(\gamma{\rm n} \to {\rm n}\eta)$	280	1.32	1.37	1.31	CB-ELSA
$\Sigma(\gamma{\rm n} \to {\rm n}\eta)$	88	1.75	2.07	1.79	GRAAL
$\sigma(\gamma{\rm n} \to {\rm n}\pi^0)$	147	2.01	2.48	2.03	SAID database
$\Sigma(\gamma{\rm n} \to {\rm n}\pi^0)$	28	1.02	0.95	0.90	GRAAL

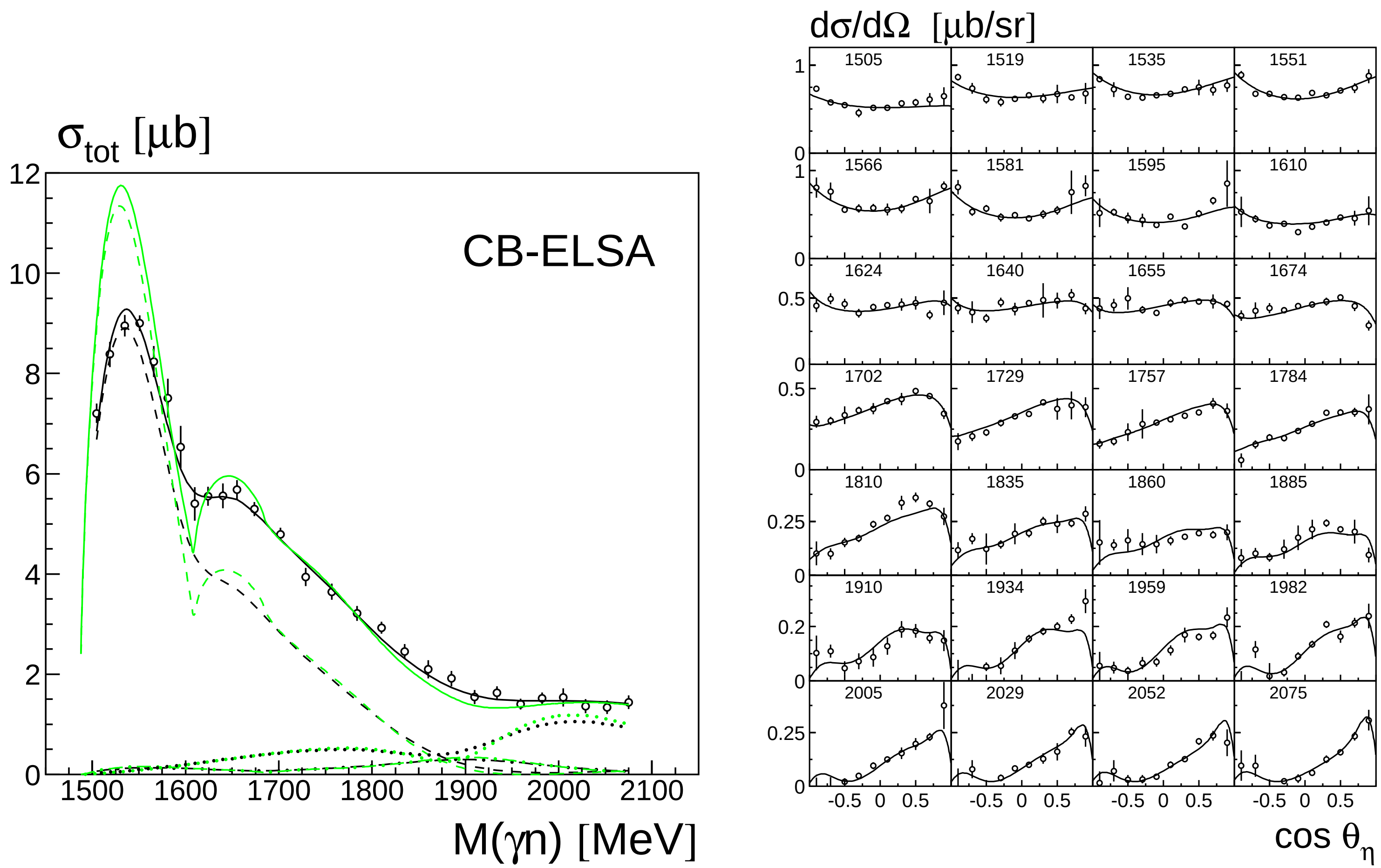

The total and differential cross section for the reaction $\gamma n \to \eta n$ obtained on the deuteron target.

The PWA result from the solution with S_{11} interference (solution 1) is shown. The green curves show the corresponding cross sections on the free neutron target (no Fermi motion).

Contributions: S_{11} (dashed), P_{13} (dotted) and P_{11} (dash-dotted)

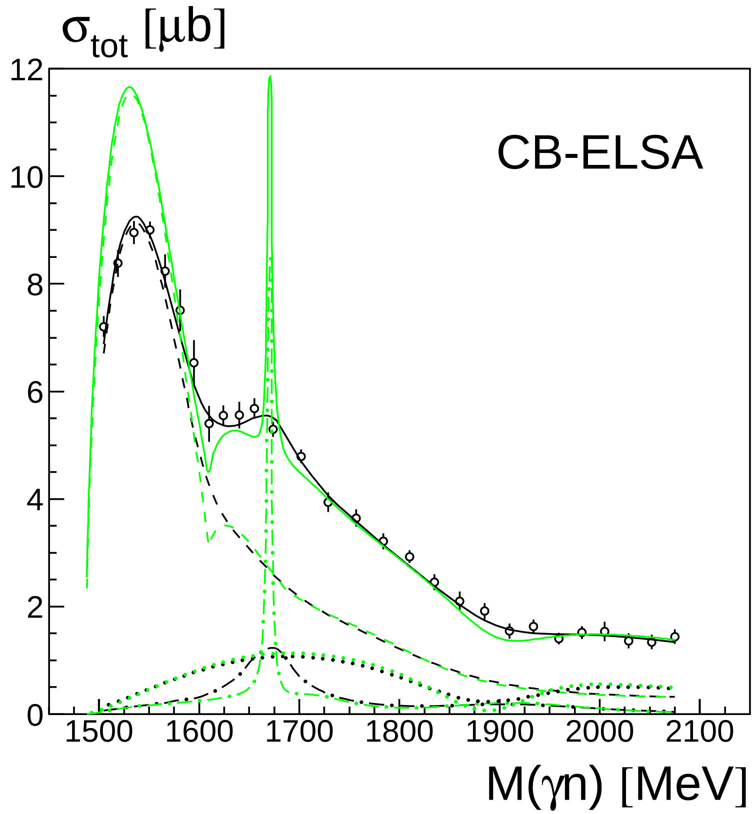

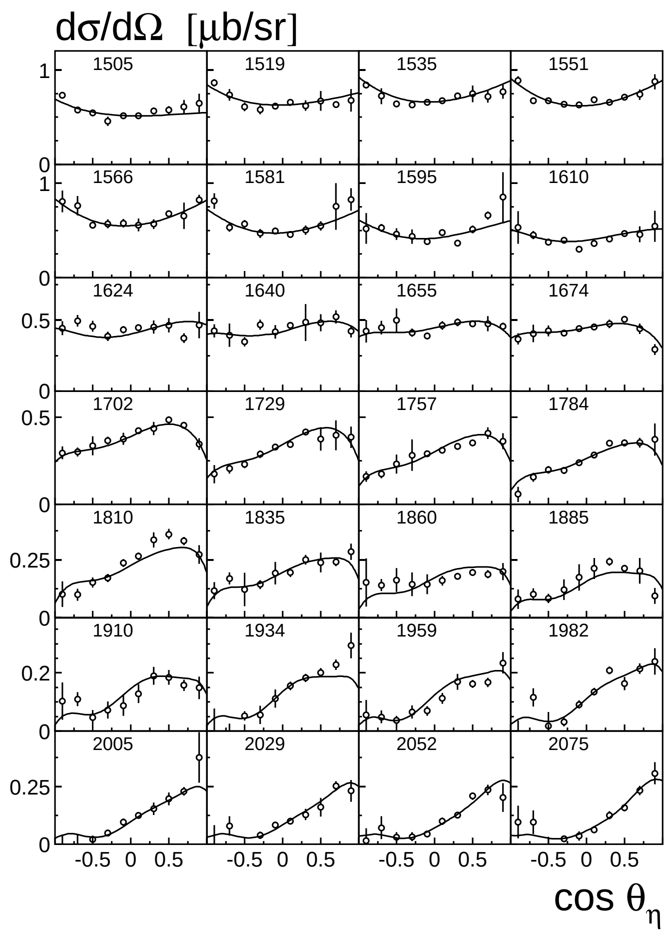

The total and differential cross section for the reaction $\gamma n \to \eta n$ obtained on the deuteron target. The PWA result from the solution with narrow P_{11} resonance (solution 3) is shown. The green curves show the corresponding cross sections on the free neutron target (no Fermi motion). Contributions: S_{11} (dashed), P_{13} (dotted) and P_{11} (dash-dotted)

Beam asymmetry for the $\gamma n \to \eta n$ and $\gamma n \to \pi^0 n$

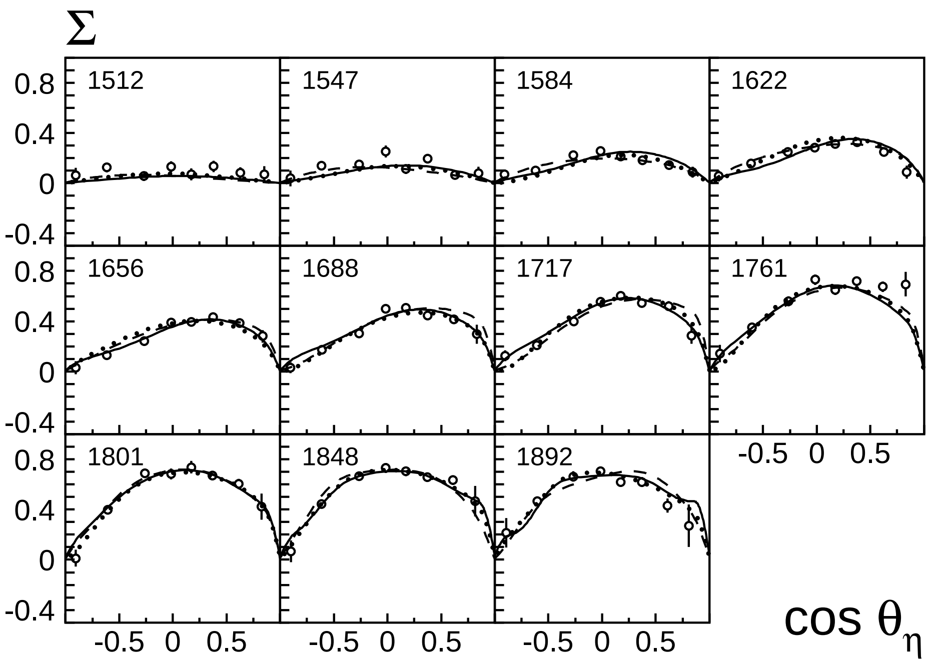

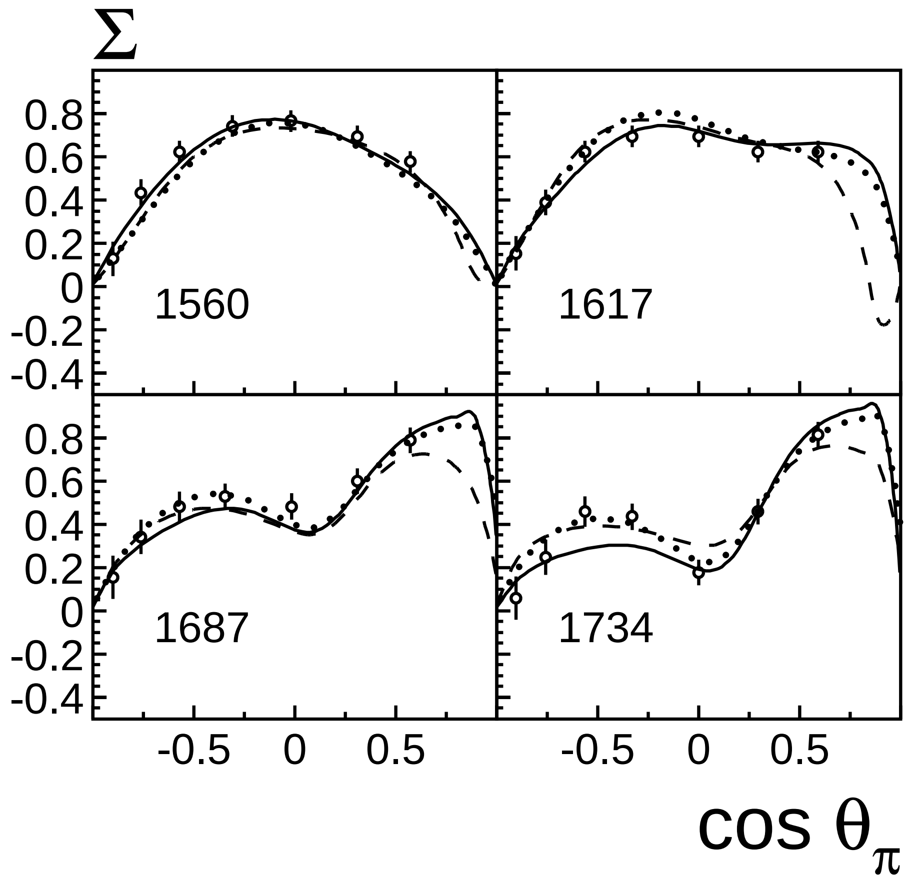

Beam asymmetry for the $\gamma p \to \eta p$ with fine bins

Solution 1: $\chi^2 = 1.35$ **Solution 3:** $\chi^2 = 0.95$

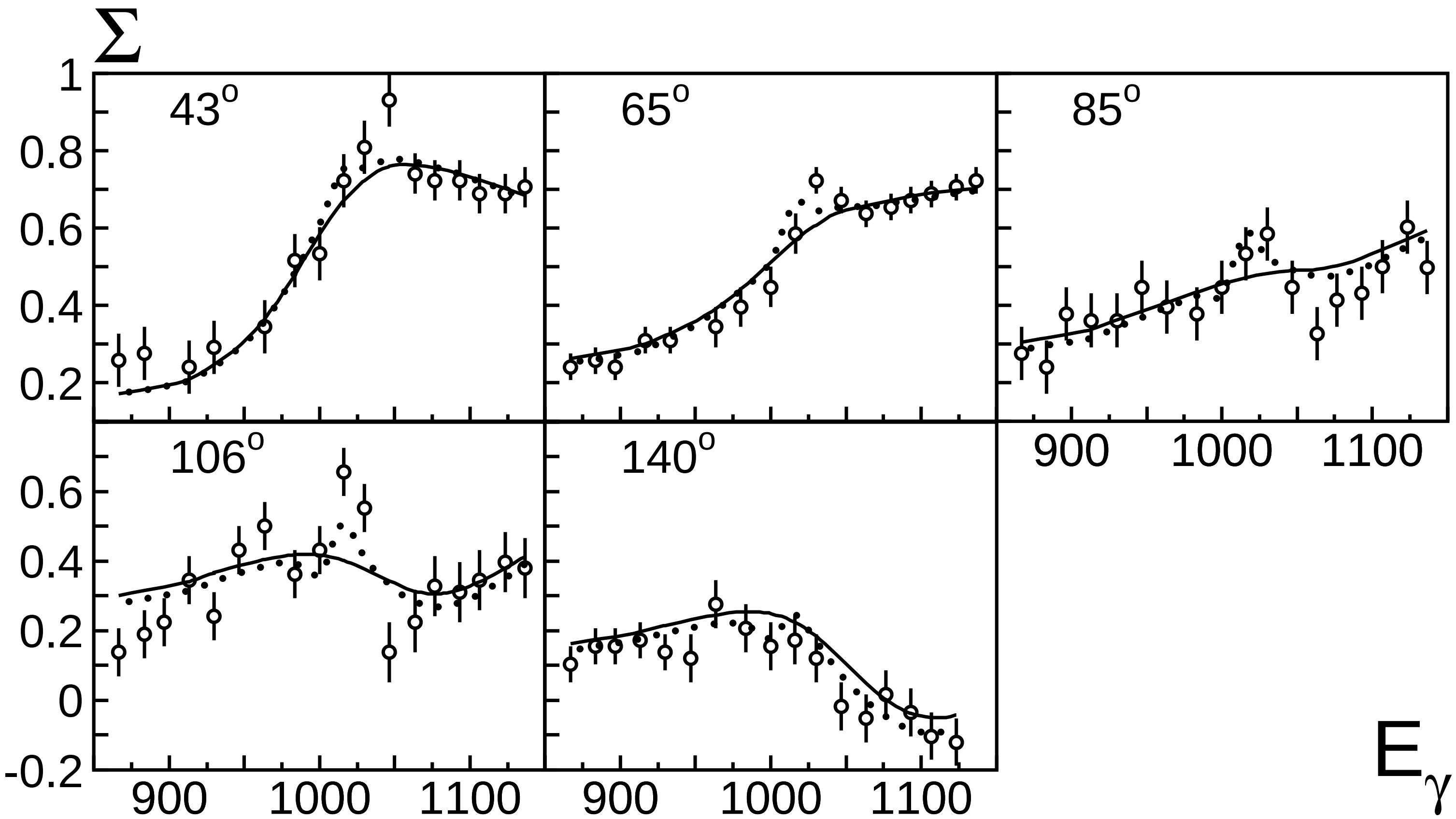

The long-standing discrepancies between the photo-production amplitude $A^n_{1/2}$ for $N(1535)S_{11}$ production ($A^n_{1/2} = -0.020 \pm 0.035$ GeV$^{-1/2}$ from $\gamma n \to n\pi^0$ (Arndt); $A^n_{1/2} = -0.100 \pm 0.030$ GeV$^{-1/2}$ from $\gamma n \to n\eta$ (Krusche) is solved.

	$S_{11}(1535)$	$S_{11}(1650)$
Pole position (mass)	1.505 ± 0.020	1.640 ± 0.015
(width)	0.145 ± 0.025	0.165 ± 0.015
PDG	1.510 ± 0.020	1.655 ± 0.015
	0.170 ± 0.080	0.165 ± 0.015
$A^p_{1/2}$ **(GeV**$^{-1/2}$)	0.090 ± 0.025	0.100 ± 0.035
PDG	0.090 ± 0.030	0.053 ± 0.016
phase	$(20 \pm 15)^\circ$	$(25 \pm 20)^\circ$
$A^n_{1/2}$ **(GeV**$^{-1/2}$)	-0.080 ± 0.020	-0.055 ± 0.020
PDG	-0.046 ± 0.027	-0.015 ± 0.021
phase	$(20 \pm 20)^\circ$	$(30 \pm 25)^\circ$

Summary

1. An approach for the combined analysis of the pion and photo induced reaction with two and multi particle final states is developed.
2. The combined analysis of more them 45 different reactions helped to identify the properties of known baryons.
3. The analysis of the data on hyperon photoproduction reveal two new baryon states in the region of 1900 MeV, $P_{11}(1880)$ and $P_{13}(1900)$.
4. The η-photoproduction data reveal the baryon resonance $D_{15}(2070)$.
5. The $D_{33}(1940)$ state is needed for the description of the $\gamma p \to \pi^0 \eta p$ data.
6. The structure at 1670 MeV observed in the η photoproduction data off neutron can be explained either by the interference within S_{11} wave or by a contribution of a narrow P_{11} state with mass 1670 ± 6 MeV. No other mechanism can explain this reaction.
7. The spectrum of observed states is in direct contradiction with a classical quark model. The best explanations are chiral symmetry restoration or AdS/QCD soft-wall

model.